

AUGMENTED FINITE ELEMENT FORMULATION FOR THE NAVIER–STOKES EQUATIONS WITH VORTICITY AND VARIABLE VISCOSITY

VERONICA ANAYA¹, RUBEN CARABALLO², RICARDO RUIZ-BAIER³ AND HECTOR TORRES⁴

Abstract. We propose and analyse an augmented mixed finite element method for the Navier–Stokes equations written in terms of velocity, vorticity, and pressure with non-constant viscosity and no-slip boundary conditions. The weak formulation includes least-squares terms arising from the constitutive equation and from the incompressibility condition, and we use a fixed point strategies to show the existence and uniqueness of continuous and discrete solutions under the assumption of sufficiently small data. The method is constructed using any compatible finite element pair for velocity and pressure as dictated by Stokes inf-sup stability, while for vorticity any generic discrete space (of arbitrary order) can be used. We establish optimal a priori error estimates. Finally, we provide a set of numerical tests in 2D and 3D illustrating the behaviour of the scheme as well as verifying the theoretical convergence rates.

2020 Mathematics Subject Classification. 65N30, 65N12, 76D07, 65N15.

Updated: November 30, 2021.

1. INTRODUCTION

1.1. Scope

Incompressible flow equations in vorticity formulation play a critical role in describing rotational flows in a natural way. A diversity of formulations are available from the relevant literature. Of particular interest to us is their formulation in terms of velocity, vorticity (the curl of velocity), and pressure. These variables were used for Stokes and Navier–Stokes flows in the seminal papers [21, 23, 27, 28], which analyse unique solvability and propose conforming discretisations. That form has led to a number of generalisations in Brinkman, Oseen, and Navier–Stokes equations and exploring different types of discretisation approaches including mixed finite element [5, 12, 13, 44], stabilised [4, 43], least-squares [10, 20, 45], discontinuous Galerkin [8], adaptive, hybrid discontinuous Galerkin [24], spectral [1, 15, 17, 26], and preconditioned methods [46].

Similarly to these references, in the present work we are interested in the Navier–Stokes equations written in terms of velocity, vorticity, and pressure. However the present work considers the case of variable kinematic viscosity, for which the formulations above are not applicable since the viscous contribution to stress cannot be

Keywords and phrases: Navier–Stokes equations; vorticity-based formulation; mixed finite elements; non-constant viscosity; a priori error analysis.

¹ GIMNAP, Departamento de Matemática, Universidad del Bío-Bío, Casilla 5-C, Concepción, Chile; and Centro de Investigación en Ingeniería Matemática (CI²MA), Universidad de Concepción, Chile.
E-mail: vanaya@ubiobio.cl.

² Corresponding author. GIMNAP, Departamento de Matemática, Universidad del Bío-Bío, Casilla 5-C, Concepción, Chile.
E-mail: ruben.caraballo1801@alumnos.ubiobio.cl.

³ School of Mathematics, Monash University, 9 Rainforest Walk, Melbourne, VIC 3800, Australia; and Institute of Computer Science and Mathematical Modelling, Sechenov University, Moscow, Russian Federation; and Research Core on Natural and Exact Sciences, Universidad Adventista de Chile, Casilla 7-D, Chillán, Chile.
E-mail: ricardo.ruizbaier@monash.edu.

⁴ Departamento de Matemáticas, Universidad de La Serena, La Serena, Chile.
E-mail: htorres@userena.cl.

easily split in the usual rotation form (because, in general, $-\operatorname{div}(\nu \nabla \mathbf{u}) \neq \nu \operatorname{curl}(\operatorname{curl} \mathbf{u}) - \nu \nabla(\operatorname{div} \mathbf{u})$). Such an addition (and addressed for vorticity-based Stokes, Brinkman, and Oseen formulations in [9, 11, 29]) yields a non-symmetric variational form that can be augmented using residual terms from the constitutive and mass conservation equations. In the present treatment, additional terms appear due to the variable viscosity, which require a regularity assumption on the viscosity gradient. In [11] the kinematic viscosity ν is assumed in $W^{1,\infty}(\Omega)$, and in the Darcy–heat system analysed in [18] the viscosity is assumed Lipschitz continuous. For our analysis it suffices to take $\nu \in W^{1,r^*}(\Omega)$, with $r^* = \frac{2r}{r-2}$, and $r \in (2, 6]$ for 3D and $r \in (2, \infty)$ for 2D. For example, $\nu \in W^{1,3}(\Omega)$ in 2D or 3D.

The extension to the Navier–Stokes case is carried out in this paper. The unique solvability in the constant viscosity case can be established as in [15, 26], utilising antisymmetry of the convection term, appropriate continuity properties, smallness assumption on data, embeddings in separable Hilbert spaces, constructing sequences of finite-dimensional spaces, and Brouwer’s fixed-point theorem. In our case the solvability analysis follows by a combination of Banach fixed-point theory using the velocity as fixed-point variable, and classical Babuška–Brezzi theory for saddle-point problems (by grouping together the velocity and vorticity unknowns). For this we have drawn inspiration from the analysis of Navier–Stokes–Darcy from the recent work [31]. The second aim of this paper is to construct a family of conforming discretisations. We can use simply Stokes-stable elements for velocity and pressure, while the vorticity can be approximated with arbitrary elements. For example, if choosing continuous or discontinuous piecewise polynomials of the same polynomial degree as pressure, we get an overall optimally convergent method with the same rates in all variables.

Of note, a number of differences with respect to rotational Oseen and Navier–Stokes equations are inherited from the augmentation. First, the convective term is written in the usual way for the standard velocity–pressure formulation, $(\nabla \mathbf{u})\mathbf{u}$, rather than in the rotational form $\operatorname{curl} \mathbf{u} \times \mathbf{u}$. This implies that we do not need to use the Bernoulli pressure (a nonlinear function of velocity module and kinematic pressure) to treat the momentum equation [16, 36–38]. Secondly, as in [10] one counts with higher velocity regularity than the usual $H(\operatorname{div}, \Omega)$ typically achieved in the formulations in the former list of references (this feature facilitates the analysis when manipulating the advecting term, but it comes at the expense of giving up the exact satisfaction of the divergence-free constraint at discrete level). Third, the augmentation permits us to obtain a higher convergence rate for vorticity, and it allows us to easily impose no-slip velocity conditions. Another advantage of the present formulation is that it accommodates generalisations to non-isothermal systems and the coupling with other transport effects in the very relevant case where viscosity depends on concentration or temperature [39, 40, 42].

1.2. Outline

The contents of the paper have been organised as follows. Functional spaces and recurrent notation will be recalled and we will present the governing equations in terms of velocity, vorticity and pressure, and state the augmented formulation to the Navier–Stokes problem. The solvability analysis is presented in Section 2. The tools used therein are standard fixed point arguments. The Galerkin discretisation is presented in Section 3, where we also derive the stability analysis. Convergence rates for particular finite element subspaces including Taylor–Hood, Bernardi–Raugel, and MINI-elements are given in Section 3.3. We visit several numerical tests illustrating the convergence of the proposed method under different scenarios (including cases not covered by our analysis) are reported in Section 4, and we close with a summary of our findings as well as concluding remarks laid out in Section 5.

1.3. Vorticity-based Navier–Stokes equations

Let Ω be a bounded domain of \mathbb{R}^d , $d = 2, 3$, with Lipschitz boundary $\Gamma = \partial\Omega$. For any $s \geq 0$, the notation $\|\cdot\|_{s,\Omega}$ stands for the norm of the Hilbertian Sobolev spaces $H^s(\Omega)$ or $H^s(\Omega)^d$, with the usual convention $H^0(\Omega) := L^2(\Omega)$. All through this paper C will represent some absolute constant varying line by line.

Let us consider the Navier–Stokes problem with non-constant viscosity modelling the steady-state flow of an incompressible viscous fluid. The governing equations can be rewritten using the velocity \mathbf{u} , the vorticity $\boldsymbol{\omega}$ and the pressure p as follows (cf. [4, 7, 20]): Given a sufficiently smooth force density \mathbf{f} , we seek $(\mathbf{u}, \boldsymbol{\omega}, p)$ such that

$$\sigma \mathbf{u} + \nu \operatorname{curl} \boldsymbol{\omega} + (\mathbf{u} \cdot \nabla) \mathbf{u} - 2\varepsilon(\mathbf{u}) \nabla \nu + \nabla p = \mathbf{f} \quad \text{in } \Omega, \quad (1.1a)$$

$$\boldsymbol{\omega} - \operatorname{curl} \mathbf{u} = \mathbf{0} \quad \text{in } \Omega, \quad (1.1b)$$

$$\operatorname{div} \mathbf{u} = 0 \quad \text{in } \Omega, \quad (1.1c)$$

$$\mathbf{u} = \mathbf{0} \quad \text{on } \Gamma, \quad (1.1d)$$

$$(p, 1)_{0,\Omega} = 0. \quad (1.1e)$$

In the model the kinematic viscosity of the fluid is assumed such that $\nu \in W^{1,r^*}(\Omega)$ (with r^* made precise in (2.1) below) and $0 < \nu_0 \leq \nu \leq \nu_1$. Moreover, the coefficient $\sigma : \Omega \rightarrow \mathbb{R}$ satisfies $0 < \sigma_0 \leq \sigma(x) \leq \sigma_1$. In the context of Navier–Stokes/Brinkman flows, it represents the inverse of the permeability scaled with viscosity. In addition, we will assume that $\mathbf{f} \in L^2(\Omega)^d$. The precise derivation and analysis of non-standard types of boundary conditions for the usual velocity–vorticity–pressure formulation is a delicate matter. We do not address it here and simply consider no-slip conditions for velocity everywhere on Γ .

Equation (1.1a) results from using the following, point-wisely satisfied, useful vector identity

$$\operatorname{curl}(\operatorname{curl} \mathbf{v}) = -\Delta \mathbf{v} + \nabla(\operatorname{div} \mathbf{v}),$$

and noting that the velocity \mathbf{u} is solenoidal, we have the chain of identities

$$-2 \operatorname{div}(\nu \boldsymbol{\varepsilon}(\mathbf{u})) = -2\nu \operatorname{div}(\boldsymbol{\varepsilon}(\mathbf{u})) - 2\boldsymbol{\varepsilon}(\mathbf{u})\nabla\nu = -\nu\Delta\mathbf{u} - 2\boldsymbol{\varepsilon}(\mathbf{u})\nabla\nu = \nu \operatorname{curl}(\operatorname{curl} \mathbf{u}) - 2\boldsymbol{\varepsilon}(\mathbf{u})\nabla\nu.$$

1.4. Variational formulation

In this section, we propose a mixed variational formulation of system (1.1a)–(1.1e). First, we endow the space $H_0^1(\Omega)^d$ with the following norm:

$$\|\mathbf{v}\|_{1,\Omega}^2 := \|\mathbf{v}\|_{0,\Omega}^2 + \|\operatorname{curl} \mathbf{v}\|_{0,\Omega}^2 + \|\operatorname{div} \mathbf{v}\|_{0,\Omega}^2.$$

We note that, in $H_0^1(\Omega)^d$, the above norm is equivalent to the usual norm, the above equivalence is a consequence of the identity:

$$\|\nabla \mathbf{v}\|_{0,\Omega}^2 = \|\operatorname{curl} \mathbf{v}\|_{0,\Omega}^2 + \|\operatorname{div} \mathbf{v}\|_{0,\Omega}^2.$$

In the sequel it will be useful to work with the product spaces $X := H_0^1(\Omega)^d \times L^2(\Omega)^{d(d-1)/2}$ and $H := H_0^1(\Omega)^d \times L^2(\Omega)^{d(d-1)/2} \times L_0^2(\Omega)$ equipped with the norms

$$\|(\mathbf{v}, \boldsymbol{\theta})\|_X^2 := \|\mathbf{v}\|_{1,\Omega}^2 + \|\boldsymbol{\theta}\|_{0,\Omega}^2 \quad \text{and} \quad \|(\mathbf{v}, \boldsymbol{\theta}, q)\|_H^2 := \|(\mathbf{v}, \boldsymbol{\theta})\|_X^2 + \|q\|_{0,\Omega}^2,$$

respectively. To derive a weak formulation we multiply by suitable test functions, integrate over the domain and apply the usual integration by parts as well as the following version of Green’s formula from e.g. [33, Theorem 2.11]:

$$(\operatorname{curl} \boldsymbol{\omega}, \mathbf{v})_{0,\Omega} = (\boldsymbol{\omega}, \operatorname{curl} \mathbf{v})_{0,\Omega} + \langle \boldsymbol{\omega} \times \mathbf{n}, \mathbf{v} \rangle_{0,\Gamma}.$$

We arrive at the following augmented variational formulation for the Navier–Stokes problem (1.1a)–(1.1e): Find $((\mathbf{u}, \boldsymbol{\omega}), p) \in (H_0^1(\Omega)^d \times L^2(\Omega)^{d(d-1)/2}) \times L_0^2(\Omega)$ such that

$$\begin{aligned} a((\mathbf{u}, \boldsymbol{\omega}), (\mathbf{v}, \boldsymbol{\theta})) + N(\mathbf{u}; \mathbf{u}, \mathbf{v}) + b((\mathbf{v}, \boldsymbol{\theta}), p) &= F(\mathbf{v}, \boldsymbol{\theta}) & \forall (\mathbf{v}, \boldsymbol{\theta}) \in H_0^1(\Omega)^d \times L^2(\Omega)^{d(d-1)/2}, \\ b((\mathbf{u}, \boldsymbol{\omega}), q) &= 0 & \forall q \in L_0^2(\Omega), \end{aligned} \quad (1.2)$$

where the bilinear/trilinear forms and the linear functional are defined as:

$$\begin{aligned} a((\mathbf{u}, \boldsymbol{\omega}), (\mathbf{v}, \boldsymbol{\theta})) &:= (\sigma \mathbf{u}, \mathbf{v})_{0,\Omega} + (\nu \boldsymbol{\omega}, \operatorname{curl} \mathbf{v})_{0,\Omega} - (\nu \boldsymbol{\theta}, \operatorname{curl} \mathbf{u})_{0,\Omega} + \kappa_1 (\operatorname{curl} \mathbf{u}, \operatorname{curl} \mathbf{v})_{0,\Omega} + \kappa_2 (\operatorname{div} \mathbf{u}, \operatorname{div} \mathbf{v})_{0,\Omega} \\ &\quad - \kappa_1 (\boldsymbol{\omega}, \operatorname{curl} \mathbf{v})_{0,\Omega} - 2(\boldsymbol{\varepsilon}(\mathbf{u})\nabla\nu, \mathbf{v})_{0,\Omega} + (\boldsymbol{\omega}, \nabla\nu \times \mathbf{v})_{0,\Omega}, \end{aligned} \quad (1.3)$$

$$N(\mathbf{w}; \mathbf{u}, \mathbf{v}) := ((\mathbf{w} \cdot \nabla) \mathbf{u}, \mathbf{v})_{0,\Omega}, \quad b((\mathbf{v}, \boldsymbol{\theta}), q) := -(q, \operatorname{div} \mathbf{v})_{0,\Omega}, \quad F(\mathbf{v}, \boldsymbol{\theta}) := (\mathbf{f}, \mathbf{v})_{0,\Omega},$$

for all $(\mathbf{u}, \boldsymbol{\omega}), (\mathbf{v}, \boldsymbol{\theta}) \in H_0^1(\Omega)^d \times L^2(\Omega)^{d(d-1)/2}$, and $q \in L_0^2(\Omega)$.

2. ANALYSIS OF THE CONTINUOUS VARIATIONAL FORMULATION

To establish well-posedness of the nonlinear problem (1.2) we use a fixed-point strategy. First we require some preliminary notions.

Consider fixed real numbers

$$r \in \begin{cases} (2, \infty) & \text{for } d = 2, \\ (2, 6] & \text{for } d = 3, \end{cases} \quad \text{and} \quad r^* = \frac{2r}{r-2}, \quad (2.1)$$

to be used when estimating terms of the form $(\boldsymbol{\omega}, \nabla \nu \times \mathbf{v})_{0,\Omega}$.

We continue by recalling the following Sobolev inequality (see [2]),

$$\|\phi\|_{0,r,\Omega} \leq C_r \|\phi\|_{1,\Omega}, \quad \forall \phi \in H^1(\Omega). \quad (2.2)$$

Then, we see from (2.2) that

$$\|\mathbf{v}\|_{0,r,\Omega} \leq C_r d^{\frac{r-2}{2r}} \|\mathbf{v}\|_{1,\Omega}, \quad \forall \mathbf{v} \in H^1(\Omega)^d, \quad (2.3)$$

which implies that

$$|N(\boldsymbol{\beta}; \mathbf{u}, \mathbf{v})| = |((\boldsymbol{\beta} \cdot \nabla) \mathbf{u}, \mathbf{v})_{0,\Omega}| \leq C_4^2 d^{1/2} \|\boldsymbol{\beta}\|_{1,\Omega} \|\mathbf{u}\|_{1,\Omega} \|\mathbf{v}\|_{1,\Omega}, \quad (2.4)$$

for all $\boldsymbol{\beta}, \mathbf{v}, \mathbf{u} \in H^1(\Omega)^d$. Next, using the identity

$$N(\boldsymbol{\beta}; \mathbf{u}, \mathbf{v}) + N(\boldsymbol{\beta}; \mathbf{v}, \mathbf{u}) = ((\boldsymbol{\beta} \cdot \nabla) \cdot \mathbf{u}, \mathbf{v})_{0,\Omega} + ((\boldsymbol{\beta} \cdot \nabla) \mathbf{v}, \mathbf{u})_{0,\Omega} = -(\operatorname{div} \boldsymbol{\beta}, \mathbf{u} \cdot \mathbf{v})_{0,\Omega},$$

we can deduce from (2.3) that

$$|N(\boldsymbol{\beta}; \mathbf{v}, \mathbf{v})| = |((\boldsymbol{\beta} \cdot \nabla) \mathbf{v}, \mathbf{v})_{0,\Omega}| \leq \frac{C_4^2 d^{1/2}}{2} \|\operatorname{div} \boldsymbol{\beta}\|_{0,\Omega} \|\mathbf{v}\|_{1,\Omega}^2, \quad \forall \boldsymbol{\beta}, \mathbf{v} \in H^1(\Omega)^d.$$

The following inf-sup condition holds (cf. [30]). There exists $C > 0$, depending only on Ω , such that

$$\sup_{0 \neq \mathbf{v} \in H_0^1(\Omega)^d} \frac{|(q, \operatorname{div} \mathbf{v})_{0,\Omega}|}{\|\mathbf{v}\|_{1,\Omega}} \geq C \|q\|_{0,\Omega} \quad \forall q \in L_0^2(\Omega).$$

As a consequence, we immediately have the following lemma.

Lemma 2.1. *There exists $\gamma > 0$, independent of ν , such that*

$$\sup_{0 \neq (\mathbf{v}, \boldsymbol{\theta}) \in X} \frac{|b((\mathbf{v}, \boldsymbol{\theta}), q)|}{\|(\mathbf{v}, \boldsymbol{\theta})\|_X} \geq \gamma \|q\|_{0,\Omega} \quad \forall q \in L_0^2(\Omega).$$

Next, and similarly as in [9], we can readily state the following collection of results.

Lemma 2.2. *Let $\kappa_1, \kappa_2 > 0$ with $0 < \kappa_1 < \frac{2}{3}\nu_0$, and assume that $\boldsymbol{\beta} \in H^1(\Omega)^d$ and*

$$C_r^2 d^{\frac{r-2}{r}} \|\nabla \nu\|_{0,r^*,\Omega}^2 \left\{ \frac{1}{\kappa} + \frac{3}{\nu_0} \right\} + \frac{C_4^2 d^{1/2}}{2} \|\operatorname{div} \boldsymbol{\beta}\|_{0,\Omega} < \min \left\{ \sigma_0, \frac{\kappa_2}{2}, \kappa_1 - \frac{3\kappa_1^2}{4\nu_0} \right\},$$

where $\kappa = \min\{\kappa_1, \kappa_2\}$. Then, the bilinear/trilinear forms defined in (1.3) are bounded

$$\|a\| \leq A_0 A_1, \quad \|b\| \leq 1, \quad \|F\| \leq \|\mathbf{f}\|_{0,\Omega}, \quad \|a + N(\boldsymbol{\beta}; \cdot, \cdot)\| \leq B_0(\boldsymbol{\beta}) B_1(\boldsymbol{\beta}),$$

with

$$\begin{aligned} A_0 &= \max\{\sigma_1, \nu_1 + \kappa_1, \max\{\kappa_2, \nu_1 + \kappa_1\} + 2C_r d^{\frac{r-2}{2r}} \|\nabla \nu\|_{0,r^*,\Omega}\}^{1/2}, \\ A_1 &= \max\{\nu_1 + 2C_r d^{\frac{r-2}{2r}} \|\nabla \nu\|_{0,r^*,\Omega}, \max\{\sigma_1, \kappa_2, \nu_1 + 2\kappa_1\} + 4C_r d^{\frac{r-2}{2r}} \|\nabla \nu\|_{0,r^*,\Omega}\}^{1/2}, \\ B_0(\boldsymbol{\beta}) &= \max\{\sigma_1, \nu_1 + \kappa_1, \max\{\kappa_2, \nu_1 + \kappa_1\} + 2C_r d^{\frac{r-2}{2r}} \|\nabla \nu\|_{0,r^*,\Omega} + C_4^2 d^{1/2} \|\boldsymbol{\beta}\|_{1,\Omega}\}^{1/2}, \end{aligned}$$

$$B_1(\boldsymbol{\beta}) = \max\{\nu_1 + 2C_r d^{\frac{r-2}{2r}} \|\nabla \nu\|_{0,r^*,\Omega}, \max\{\sigma_1, \kappa_2, \nu_1 + 2\kappa_1\} + 4C_r d^{\frac{r-2}{2r}} \|\nabla \nu\|_{0,r^*,\Omega} + C_4^2 d^{1/2} \|\boldsymbol{\beta}\|_{1,\Omega}\}^{1/2}.$$

Moreover, for a $\boldsymbol{\beta}$ given, the bilinear form $a(\cdot, \cdot) + N(\boldsymbol{\beta}; \cdot, \cdot)$ is elliptic

$$a((\mathbf{v}, \boldsymbol{\theta}), (\mathbf{v}, \boldsymbol{\theta})) + N(\boldsymbol{\beta}; \mathbf{v}, \mathbf{v}) \geq \widehat{\alpha}(\boldsymbol{\beta}) \|(\mathbf{v}, \boldsymbol{\theta})\|_X^2 \quad \forall (\mathbf{v}, \boldsymbol{\theta}) \in X,$$

where $\widehat{\alpha}(\boldsymbol{\beta}) := \widehat{\alpha}(\sigma_0, \nu, \kappa_2, \boldsymbol{\beta}) = \min\{\frac{\nu_0}{3}, \lambda\}$ with

$$\lambda := \min\left\{\sigma_0, \frac{\kappa_2}{2}, \kappa_1 - \frac{3\kappa_1^2}{4\nu_0}\right\} - C_r^2 d^{\frac{r-2}{r}} \|\nabla \nu\|_{0,r^*,\Omega}^2 \left\{\frac{1}{\kappa} + \frac{3}{\nu_0}\right\} - \frac{C_4^2 d^{1/2}}{2} \|\operatorname{div} \boldsymbol{\beta}\|_{0,\Omega}.$$

Lemma 2.3. *There exists $(\mathbf{u}, \boldsymbol{\omega}, p) \in \mathbf{H}_0^1(\Omega)^d \times \mathbf{L}^2(\Omega)^{d(d-1)/2} \times \mathbf{L}_0^2(\Omega)$ such that*

$$\begin{aligned} a((\mathbf{u}, \boldsymbol{\omega}), (\mathbf{v}, \boldsymbol{\theta})) + N(\boldsymbol{\beta}; \mathbf{u}, \mathbf{v}) + b((\mathbf{v}, \boldsymbol{\theta}), p) &= F(\mathbf{v}, \boldsymbol{\theta}) \quad \forall (\mathbf{v}, \boldsymbol{\theta}) \in \mathbf{H}_0^1(\Omega)^d \times \mathbf{L}^2(\Omega)^{d(d-1)/2}, \\ b((\mathbf{u}, \boldsymbol{\omega}), q) &= 0 \quad \forall q \in \mathbf{L}_0^2(\Omega). \end{aligned} \quad (2.5)$$

In addition, the solution satisfies the following continuous dependence on data

$$\|(\mathbf{u}, \boldsymbol{\omega})\|_X \leq \frac{\|\mathbf{f}\|_{0,\Omega}}{\widehat{\alpha}(\boldsymbol{\beta})}, \quad \|p\|_{0,\Omega} \leq \gamma^{-1} \left(1 + \frac{\|a + N(\boldsymbol{\beta}; \cdot, \cdot)\|}{\widehat{\alpha}(\boldsymbol{\beta})}\right) \|\mathbf{f}\|_{0,\Omega}.$$

Lemmas 2.2 and 2.3 will be used in showing the existence of a fixed point, stated as follows.

Lemma 2.4. *Let $\kappa_1, \kappa_2 > 0$ with $0 < \kappa_1 < \frac{2}{3}\nu_0$, and suppose that*

$$C_r^2 d^{\frac{r-2}{r}} \|\nabla \nu\|_{0,r^*,\Omega}^2 \left\{\frac{1}{\kappa} + \frac{3}{\nu_0}\right\} < \min\left\{\sigma_0, \frac{\kappa_2}{2}, \kappa_1 - \frac{3\kappa_1^2}{4\nu_0}\right\}. \quad (2.6)$$

Consider the set

$$\mathcal{O} := \{\mathbf{u} \in \mathbf{H}_0^1(\Omega)^d : \|\mathbf{u}\|_{1,\Omega} \leq \delta\},$$

defined by choosing $0 < \delta < \frac{\bar{\alpha}}{C_4^2 d^{1/2}}$ with

$$\alpha := \alpha(\sigma_0, \nu, \kappa_1, \kappa_2) = \min\left\{\sigma_0, \frac{\kappa_2}{2}, \kappa_1 - \frac{3\kappa_1^2}{4\nu_0}\right\} - C_r^2 d^{\frac{r-2}{r}} \|\nabla \nu\|_{0,r^*,\Omega}^2 \left\{\frac{1}{\kappa} + \frac{3}{\nu_0}\right\},$$

and $\bar{\alpha} := \min\{\frac{\nu_0}{3}, \alpha\}$. If

$$\|\mathbf{f}\|_{0,\Omega} < \frac{1}{2}\bar{\alpha}\delta, \quad (2.7)$$

then, the operator $\mathcal{J} : \mathcal{O} \rightarrow \mathcal{O}$, with $\boldsymbol{\beta} \mapsto \mathcal{J}(\boldsymbol{\beta}) = \mathbf{u}$ (and where \mathbf{u} is the velocity solution of the Oseen problem (2.5), for a $\boldsymbol{\beta}$ given), has a unique fixed point in \mathcal{O} .

Proof. From the assumptions (2.6)-(2.7) it follows that \mathcal{J} is well-defined in \mathcal{O} .

Next, we note that for all $\boldsymbol{\beta} \in \mathcal{O}$, the following chain of bounds holds

$$\frac{\|\mathbf{f}\|_{0,\Omega}}{\delta} + \frac{C_4^2 d^{1/2}}{2} \|\operatorname{div} \boldsymbol{\beta}\|_{0,\Omega} \leq \frac{\|\mathbf{f}\|_{0,\Omega}}{\delta} + \frac{C_4^2 d^{1/2}}{2} \|\boldsymbol{\beta}\|_{1,\Omega} \leq \frac{1}{2}\alpha + \frac{C_4^2 d^{1/2}\delta}{2} < \alpha,$$

and consequently

$$\|\mathcal{J}(\boldsymbol{\beta})\|_{1,\Omega} \leq \frac{\|\mathbf{f}\|_{0,\Omega}}{\widehat{\alpha}(\boldsymbol{\beta})} < \delta,$$

which implies that $\mathcal{J}(\mathcal{O}) \subset \mathcal{O}$.

Now, we have to prove that \mathcal{J} is a contraction. In fact, for each $i \in \{1, 2\}$ suppose that we have $\mathcal{J}(\boldsymbol{\beta}_i) = \mathbf{u}_i$. Therefore, for each triplet $(\mathbf{v}, \boldsymbol{\theta}, q) \in \mathbf{H}_0^1(\Omega)^d \times \mathbf{L}^2(\Omega)^{d(d-1)/2} \times \mathbf{L}_0^2(\Omega)$ we have that

$$a((\mathbf{u}_1 - \mathbf{u}_2, \boldsymbol{\omega}_1 - \boldsymbol{\omega}_2), (\mathbf{v}, \boldsymbol{\theta})) + b((\mathbf{v}, \boldsymbol{\theta}), p_1 - p_2) = N(\boldsymbol{\beta}_2; \mathbf{u}_2, \mathbf{v}) - N(\boldsymbol{\beta}_1; \mathbf{u}_1, \mathbf{v}), \quad (2.8a)$$

$$b((\mathbf{u}_1 - \mathbf{u}_2, \boldsymbol{\omega}_1 - \boldsymbol{\omega}_2), q) = 0. \quad (2.8b)$$

On the other hand, it is evident that

$$-N(\boldsymbol{\beta}_1; \mathbf{u}_1, \mathbf{v}) + N(\boldsymbol{\beta}_2; \mathbf{u}_2, \mathbf{v}) = N(\boldsymbol{\beta}_2 - \boldsymbol{\beta}_1; \mathbf{u}_1, \mathbf{v}) + N(\boldsymbol{\beta}_2; \mathbf{u}_2 - \mathbf{u}_1, \mathbf{v}),$$

and using the triangle inequality together with the bound (2.4) we obtain

$$-N(\boldsymbol{\beta}_1; \mathbf{u}_1, \mathbf{v}) + N(\boldsymbol{\beta}_2; \mathbf{u}_2, \mathbf{v}) \leq C_4^2 d^{1/2} (\|\boldsymbol{\beta}_1 - \boldsymbol{\beta}_2\|_{1,\Omega} \|\mathbf{u}_1\|_{1,\Omega} \|\mathbf{v}\|_{1,\Omega} + \|\boldsymbol{\beta}_2\|_{1,\Omega} \|\mathbf{u}_2 - \mathbf{u}_1\|_{1,\Omega} \|\mathbf{v}\|_{1,\Omega}).$$

In turn, taking $\mathbf{v} = \mathbf{u}_2 - \mathbf{u}_1$, $\boldsymbol{\theta} = \boldsymbol{\omega}_2 - \boldsymbol{\omega}_1$ and using the equalities (2.8a)-(2.8b), we can assert that

$$\bar{\alpha} \|(\mathbf{u}_1 - \mathbf{u}_2, \boldsymbol{\omega}_1 - \boldsymbol{\omega}_2)\|_X^2 \leq C_4^2 d^{1/2} (\|\boldsymbol{\beta}_1 - \boldsymbol{\beta}_2\|_{1,\Omega} \|\mathbf{u}_1\|_{1,\Omega} \|\mathbf{u}_1 - \mathbf{u}_2\|_{1,\Omega} + \|\boldsymbol{\beta}_2\|_{1,\Omega} \|\mathbf{u}_2 - \mathbf{u}_1\|_{1,\Omega}^2),$$

and from the above inequality and the definition of \mathcal{O} , we get

$$\bar{\alpha} \|(\mathbf{u}_1 - \mathbf{u}_2, \boldsymbol{\omega}_1 - \boldsymbol{\omega}_2)\|_X^2 \leq C_4^2 d^{1/2} (\delta \|\boldsymbol{\beta}_1 - \boldsymbol{\beta}_2\|_{1,\Omega} \|\mathbf{u}_1 - \mathbf{u}_2\|_{1,\Omega} + \delta \|\mathbf{u}_2 - \mathbf{u}_1\|_{1,\Omega}^2).$$

Recalling the choice of δ we readily see that $\frac{C_4^2 d^{1/2} \delta \bar{\alpha}^{-1}}{1 - C_4^2 d^{1/2} \delta \bar{\alpha}^{-1}} < 1$ and using the bound

$$\|\mathbf{u}_2 - \mathbf{u}_1\|_{1,\Omega} \leq \|(\mathbf{u}_1 - \mathbf{u}_2, \boldsymbol{\omega}_1 - \boldsymbol{\omega}_2)\|_X,$$

we can conclude that

$$\|\mathbf{u}_2 - \mathbf{u}_1\|_{1,\Omega} \leq \frac{C_4^2 d^{1/2} \delta \bar{\alpha}^{-1}}{1 - C_4^2 d^{1/2} \delta \bar{\alpha}^{-1}} \|\boldsymbol{\beta}_1 - \boldsymbol{\beta}_2\|_{1,\Omega}.$$

Then \mathcal{J} is a contraction and Banach fixed-point theorem yields that there exists a unique fixed point $\mathbf{u} \in \mathcal{O}$ of \mathcal{J} . \square

Thanks to the previous result, we have the unique solvability of (1.2), stated in the following theorem.

Theorem 2.1. *Let $\mathbf{f} \in L^2(\Omega)^d$, and proceed under the assumptions of Lemma 2.4. Then the operator \mathcal{J} has a unique fixed point $\mathbf{u} \in \mathcal{O}$. Equivalently, problem (1.2) has a unique solution $(\mathbf{u}, \boldsymbol{\omega}, p) \in H_0^1(\Omega)^d \times L^2(\Omega)^{d(d-1)/2} \times L_0^2(\Omega)$ with $\mathbf{u} \in \mathcal{O}$.*

3. GALERKIN DISCRETISATION AND ERROR ESTIMATES

In this section we formulate a discrete problem associated with (1.2) taking generic finite dimensional subspaces that yield unique solvability and a Céa estimate. We also derive a priori error estimates, and provide the rate of convergence expected for some examples of well-known finite element families.

3.1. Preliminaries and unique solvability

Let $\{\mathcal{T}_h(\Omega)\}_{h>0}$ be a shape-regular family of partitions of the polygon/polyhedron $\bar{\Omega}$, by triangles / tetrahedra T of diameter h_T , with mesh size $h := \max\{h_T : T \in \mathcal{T}_h(\Omega)\}$. Given an integer $k \geq 0$ and a subset S of \mathbb{R}^d , the symbol $\mathcal{P}_k(S)$ denotes the space of polynomial functions defined in S of total degree less than or equal to k .

We consider generic finite dimensional subspaces $V_h \subseteq H_0^1(\Omega)^d$, $W_h \subseteq L^2(\Omega)^{d(d-1)/2}$ and $Q_h \subseteq L_0^2(\Omega)$ such that the following discrete inf-sup holds

$$\sup_{0 \neq (\mathbf{v}_h, \boldsymbol{\theta}_h) \in V_h \times W_h} \frac{|b((\mathbf{v}_h, \boldsymbol{\theta}_h), q_h)|}{\|(\mathbf{v}_h, \boldsymbol{\theta}_h)\|_X} \geq \gamma_0 \|q_h\|_{0,\Omega} \quad \forall q_h \in Q_h, \quad (3.1)$$

where $\gamma > 0$ is independent of h . Relation (3.1) is satisfied if (V_h, Q_h) is an inf-sup stable pair for the Stokes problem. In turn, the discrete space $W_h \subseteq L^2(\Omega)^{d(d-1)/2}$ for vorticity can be taken as a continuous or discontinuous polynomial space. Both options will be addressed.

The Galerkin problem reads: Find $(\mathbf{u}_h, \boldsymbol{\omega}_h, p_h) \in V_h \times W_h \times Q_h$ such that

$$\begin{aligned} a((\mathbf{u}_h, \boldsymbol{\omega}_h), (\mathbf{v}_h, \boldsymbol{\theta}_h)) + N(\mathbf{u}_h; \mathbf{u}_h, \mathbf{v}_h) + b((\mathbf{v}_h, \boldsymbol{\theta}_h), p_h) &= F(\mathbf{v}_h, \boldsymbol{\theta}_h) & \forall (\mathbf{v}_h, \boldsymbol{\theta}_h) \in V_h \times W_h, \\ rb((\mathbf{u}_h, \boldsymbol{\omega}_h), q_h) &= 0 & \forall q_h \in Q_h. \end{aligned} \quad (3.2)$$

As in the continuous analysis, problem (3.2) can be equivalently written as a fixed-point problem: Find $\mathbf{u}_h \in \mathcal{O}_h$ (where the discrete space is defined in (3.3)) such that

$$\mathcal{J}_h(\mathbf{u}_h) = \mathbf{u}_h,$$

where $\mathcal{J}_h : \mathcal{O}_h \subset V_h \rightarrow V_h$ is defined by $\beta_h \mapsto \mathcal{J}(\beta_h) = \mathbf{u}_h$, where $(\mathbf{u}_h, \boldsymbol{\omega}_h, p_h) \in V_h \times W_h \times Q_h$ is the unique solution of the discrete Oseen problem: Find $(\mathbf{u}_h, \boldsymbol{\omega}_h, p_h) \in V_h \times W_h \times Q_h$ such that

$$\begin{aligned} a((\mathbf{u}_h, \boldsymbol{\omega}_h), (\mathbf{v}_h, \boldsymbol{\theta}_h)) + N(\beta_h; \mathbf{u}_h, \mathbf{v}_h) + b((\mathbf{v}_h, \boldsymbol{\theta}_h), p_h) &= G(\mathbf{v}_h, \boldsymbol{\theta}_h) & \forall (\mathbf{v}_h, \boldsymbol{\theta}_h) \in V_h \times W_h, \\ b((\mathbf{u}_h, \boldsymbol{\omega}_h), q_h) &= 0 & \forall q_h \in Q_h. \end{aligned}$$

In order to show the unique solvability of (3.2), we proceed to first establish the well-definedness of the operator \mathcal{J}_h , then that $\mathcal{J}_h(\mathcal{O}_h) \subset \mathcal{O}_h$, and then that \mathcal{J}_h is a contraction.

Lemma 3.1. *Under the same assumptions as in Lemma 2.4, choose $0 < \delta < \frac{\bar{\alpha}}{C_4^2 d^{1/2}}$ and define the set*

$$\mathcal{O}_h := \{\mathbf{u}_h \in V_h : \|\mathbf{u}_h\|_{1,\Omega} \leq \delta\}. \quad (3.3)$$

If $\|f\|_{0,\Omega} < \frac{1}{2}\bar{\alpha}\delta$, then the operator \mathcal{J}_h has a unique fixed point in \mathcal{O}_h .

Proof. The proof is analogous to that of Lemma 2.4. □

And as an immediate consequence of Lemma 3.1, we have the following result.

Theorem 3.1. *Under the assumptions of Lemma 3.1, the operator \mathcal{J}_h has a unique fixed point $\mathbf{u}_h \in \mathcal{O}_h$. Equivalently, problem (3.2) has a unique solution $(\mathbf{u}_h, \boldsymbol{\omega}_h, p_h) \in V_h \times W_h \times Q_h$ satisfying $\mathbf{u}_h \in \mathcal{O}_h$.*

3.2. The Céa estimate

Our next objective is to obtain a best approximation result for (3.2). Let $(\mathbf{u}, \boldsymbol{\omega}, p)$ and $(\mathbf{u}_h, \boldsymbol{\omega}_h, p_h)$ be the unique solutions of (1.2) and (3.2), respectively. It is readily observed that the following error equation is satisfied:

$$\begin{aligned} a((e_{\mathbf{u}}, e_{\boldsymbol{\omega}}), (\mathbf{v}_h, \boldsymbol{\theta}_h)) + N(\mathbf{u}; \mathbf{u}, \mathbf{v}_h) - N(\mathbf{u}_h; \mathbf{u}_h, \mathbf{v}_h) + b((\mathbf{v}_h, \boldsymbol{\theta}_h), e_p) &= 0 & \forall (\mathbf{v}_h, \boldsymbol{\theta}_h) \in V_h \times W_h, \\ b((e_{\mathbf{u}}, e_{\boldsymbol{\omega}}), q_h) &= 0 & \forall q_h \in Q_h, \end{aligned} \quad (3.4)$$

where $e_{\mathbf{u}} := \mathbf{u} - \mathbf{u}_h$, $e_{\boldsymbol{\omega}} := \boldsymbol{\omega} - \boldsymbol{\omega}_h$, $e_p := p - p_h$, denote the corresponding errors. Given $(\mathbf{v}_h, \boldsymbol{\theta}_h, q_h) \in V_h \times W_h \times Q_h$, we decompose these errors as

$$\begin{aligned} e_{\mathbf{u}} &= \mathbf{z}_{\mathbf{u}} + \mathbf{x}_{\mathbf{u}} = (\mathbf{u} - \mathbf{v}_h) + (\mathbf{v}_h - \mathbf{u}_h), & e_{\boldsymbol{\omega}} &= \mathbf{z}_{\boldsymbol{\omega}} + \mathbf{x}_{\boldsymbol{\omega}} = (\boldsymbol{\omega} - \boldsymbol{\theta}_h) + (\boldsymbol{\theta}_h - \boldsymbol{\omega}_h), \\ e_p &= z_p + x_p = (p - q_h) + (q_h - p_h), \end{aligned}$$

where $\mathbf{x}_{\mathbf{u}} \in V_h$, $\mathbf{x}_{\boldsymbol{\omega}} \in W_h$ and $x_p \in Q_h$. With these notations in hand, we have the following main result.

Theorem 3.2. *Consider the assumptions of Lemma 2.4 and choose $0 < \delta < \frac{\bar{\alpha}}{2C_4^2 d^{1/2}}$. If $\|f\|_{0,\Omega} < \frac{1}{2}\bar{\alpha}\delta$, then there exists a positive constant C independent of h such that*

$$\|(\mathbf{u} - \mathbf{u}_h, \boldsymbol{\omega} - \boldsymbol{\omega}_h)\|_X + \|p - p_h\|_{0,\Omega} \leq C \inf_{(\mathbf{v}_h, \boldsymbol{\theta}_h, q_h) \in V_h \times W_h \times Q_h} \{\|\mathbf{u} - \mathbf{v}_h\|_{1,\Omega} + \|\boldsymbol{\omega} - \boldsymbol{\theta}_h\|_{0,\Omega} + \|p - q_h\|_{0,\Omega}\}.$$

Proof. Let $(\mathbf{v}_h, \boldsymbol{\theta}_h, q_h) \in V_h \times W_h \times Q_h$. From the definition of a , we have

$$a((e_{\mathbf{u}}, e_{\boldsymbol{\omega}}), (\mathbf{x}_{\mathbf{u}}, \mathbf{x}_{\boldsymbol{\omega}})) =$$

$$\begin{aligned}
& (\sigma e_{\mathbf{u}}, \mathbf{x}_{\mathbf{u}})_{0,\Omega} + (\nu e_{\omega}, \mathbf{x}_{\omega})_{0,\Omega} + (\nu e_{\omega}, \mathbf{curl} \mathbf{x}_{\mathbf{u}})_{0,\Omega} - (\nu \mathbf{x}_{\mathbf{u}}, \mathbf{curl} e_{\mathbf{u}})_{0,\Omega} + \kappa_1(\mathbf{curl} e_{\mathbf{u}}, \mathbf{curl} \mathbf{x}_{\mathbf{u}})_{0,\Omega} \\
& \quad + \kappa_2(\operatorname{div} e_{\mathbf{u}}, \operatorname{div} \mathbf{x}_{\mathbf{u}})_{0,\Omega} - \kappa_1(e_{\omega}, \mathbf{curl} \mathbf{x}_{\mathbf{u}})_{0,\Omega} - 2(\varepsilon(e_{\mathbf{u}})\nabla\nu, \mathbf{x}_{\mathbf{u}})_{0,\Omega} + (e_{\omega}, \nabla\nu \cdot \mathbf{x}_{\mathbf{u}})_{0,\Omega} \\
= & \sigma(\mathbf{z}_{\mathbf{u}}, \mathbf{x}_{\mathbf{u}})_{0,\Omega} + \sigma\|\mathbf{x}_{\mathbf{u}}\|_{0,\Omega}^2 + (\nu \mathbf{z}_{\omega}, \mathbf{x}_{\omega})_{0,\Omega} + (\nu \mathbf{x}_{\omega}, \mathbf{x}_{\omega})_{0,\Omega} + (\nu \mathbf{z}_{\omega}, \mathbf{curl} \mathbf{x}_{\mathbf{u}})_{0,\Omega} + (\nu \mathbf{x}_{\omega}, \mathbf{curl} \mathbf{x}_{\mathbf{u}})_{0,\Omega} \\
& \quad - (\nu \mathbf{x}_{\omega}, \mathbf{curl} \mathbf{z}_{\mathbf{u}})_{0,\Omega} - (\nu \mathbf{x}_{\omega}, \mathbf{curl} \mathbf{x}_{\mathbf{u}})_{0,\Omega} + \kappa_1(\mathbf{curl} \mathbf{z}_{\mathbf{u}}, \mathbf{curl} \mathbf{x}_{\mathbf{u}})_{0,\Omega} + \kappa_1\|\mathbf{curl} \mathbf{x}_{\mathbf{u}}\|_{0,\Omega}^2 \\
& \quad - \kappa_2(\operatorname{div} \mathbf{z}_{\mathbf{u}}, \operatorname{div} \mathbf{x}_{\mathbf{u}})_{0,\Omega} + \kappa_2\|\operatorname{div} \mathbf{x}_{\mathbf{u}}\|_{0,\Omega}^2 - \kappa_1(\mathbf{z}_{\omega}, \mathbf{curl} \mathbf{x}_{\mathbf{u}})_{0,\Omega} - \kappa_1(\mathbf{x}_{\omega}, \mathbf{curl} \mathbf{x}_{\mathbf{u}})_{0,\Omega} \\
& \quad - 2(\varepsilon(\mathbf{z}_{\mathbf{u}})\nabla\nu, \mathbf{x}_{\mathbf{u}})_{0,\Omega} - 2(\varepsilon(\mathbf{x}_{\mathbf{u}})\nabla\nu, \mathbf{x}_{\mathbf{u}})_{0,\Omega} + (\mathbf{z}_{\omega}, \nabla\nu \times \mathbf{x}_{\mathbf{u}})_{0,\Omega} + (\mathbf{x}_{\omega}, \nabla\nu \times \mathbf{x}_{\mathbf{u}})_{0,\Omega}.
\end{aligned}$$

By grouping terms, it is easy to see that

$$\begin{aligned}
a((\mathbf{x}_{\mathbf{u}}, \mathbf{x}_{\omega}), (\mathbf{x}_{\mathbf{u}}, \mathbf{x}_{\omega})) &= a((e_{\mathbf{u}}, e_{\omega}), (\mathbf{x}_{\mathbf{u}}, \mathbf{x}_{\omega})) - (\sigma \mathbf{z}_{\mathbf{u}}, \mathbf{x}_{\mathbf{u}})_{0,\Omega} - (\nu \mathbf{z}_{\omega}, \mathbf{x}_{\omega})_{0,\Omega} - (\nu \mathbf{z}_{\omega}, \mathbf{curl} \mathbf{x}_{\mathbf{u}})_{0,\Omega} \\
& \quad + (\nu \mathbf{x}_{\omega}, \mathbf{curl} \mathbf{z}_{\mathbf{u}})_{0,\Omega} - \kappa_1(\mathbf{curl} \mathbf{z}_{\mathbf{u}}, \mathbf{curl} \mathbf{x}_{\mathbf{u}})_{0,\Omega} - \kappa_2(\operatorname{div} \mathbf{z}_{\mathbf{u}}, \operatorname{div} \mathbf{x}_{\mathbf{u}})_{0,\Omega} \\
& \quad + \kappa_1(\mathbf{z}_{\omega}, \mathbf{curl} \mathbf{x}_{\mathbf{u}})_{0,\Omega} + 2(\varepsilon(\mathbf{z}_{\mathbf{u}})\nabla\nu, \mathbf{x}_{\mathbf{u}})_{0,\Omega} - (\mathbf{z}_{\omega}, \nabla\nu \times \mathbf{x}_{\mathbf{u}})_{0,\Omega}.
\end{aligned}$$

Next we invoke the ellipticity of $a(\cdot, \cdot)$, from which it follows that

$$\begin{aligned}
\bar{\alpha}\|(\mathbf{x}_{\mathbf{u}}, \mathbf{x}_{\omega})\|_X^2 &\leq a((e_{\mathbf{u}}, e_{\omega}), (\mathbf{x}_{\mathbf{u}}, \mathbf{x}_{\omega})) + \sigma\|\mathbf{z}_{\mathbf{u}}\|_{0,\Omega}\|\mathbf{x}_{\mathbf{u}}\|_{0,\Omega} + \nu_1\|\mathbf{z}_{\omega}\|_{0,\Omega}\|\mathbf{x}_{\omega}\|_{0,\Omega} + \nu_1\|\mathbf{z}_{\omega}\|_{0,\Omega}\|\mathbf{curl} \mathbf{x}_{\mathbf{u}}\|_{0,\Omega} \\
& \quad + \nu_1\|\mathbf{x}_{\omega}\|_{0,\Omega}\|\mathbf{curl} \mathbf{z}_{\mathbf{u}}\|_{0,\Omega} + \kappa_1\|\mathbf{curl} \mathbf{z}_{\mathbf{u}}\|_{0,\Omega}\|\mathbf{curl} \mathbf{x}_{\mathbf{u}}\|_{0,\Omega} + \kappa_2\|\operatorname{div} \mathbf{z}_{\mathbf{u}}\|_{0,\Omega}\|\operatorname{div} \mathbf{x}_{\mathbf{u}}\|_{0,\Omega} \\
& \quad + \kappa_1\|\mathbf{z}_{\omega}\|_{0,\Omega}\|\mathbf{curl} \mathbf{x}_{\mathbf{u}}\|_{0,\Omega} + 2C_r d^{\frac{r-2}{2r}}\|\nabla\nu\|_{0,r^*,\Omega}\|\nabla\mathbf{z}_{\mathbf{u}}\|_{0,\Omega}\|\mathbf{x}_{\mathbf{u}}\|_{1,\Omega} \\
& \quad + 2C_r d^{\frac{r-2}{2r}}\|\nabla\nu\|_{0,r^*,\Omega}\|\mathbf{z}_{\omega}\|_{0,\Omega}\|\mathbf{x}_{\mathbf{u}}\|_{1,\Omega},
\end{aligned}$$

and arranging terms, we obtain

$$\begin{aligned}
\bar{\alpha}\|(\mathbf{x}_{\mathbf{u}}, \mathbf{x}_{\omega})\|_X^2 &\leq a((e_{\mathbf{u}}, e_{\omega}), (\mathbf{x}_{\mathbf{u}}, \mathbf{x}_{\omega})) + (\sigma\|\mathbf{z}_{\mathbf{u}}\|_{0,\Omega} + 2\nu_1\|\mathbf{z}_{\omega}\|_{0,\Omega} + \nu_1\|\mathbf{curl} \mathbf{z}_{\mathbf{u}}\|_{0,\Omega} \\
& \quad + \kappa_1\|\mathbf{curl} \mathbf{z}_{\mathbf{u}}\|_{0,\Omega} + \kappa_2\|\operatorname{div} \mathbf{z}_{\mathbf{u}}\|_{0,\Omega} + \kappa_1\|\mathbf{z}_{\omega}\|_{0,\Omega} \\
& \quad + 2C_r d^{\frac{r-2}{2r}}\|\nabla\nu\|_{0,r^*,\Omega}\|\nabla\mathbf{z}_{\mathbf{u}}\|_{0,\Omega} + 2C_r d^{\frac{r-2}{2r}}\|\nabla\nu\|_{0,r^*,\Omega}\|\mathbf{z}_{\omega}\|_{0,\Omega})\|(\mathbf{x}_{\mathbf{u}}, \mathbf{x}_{\omega})\|_X.
\end{aligned}$$

In this way we can write the bound

$$\|(\mathbf{x}_{\mathbf{u}}, \mathbf{x}_{\omega})\|_X^2 \leq \bar{\alpha}^{-1}a((e_{\mathbf{u}}, e_{\omega}), (\mathbf{x}_{\mathbf{u}}, \mathbf{x}_{\omega})) + (m_1\|\mathbf{z}_{\omega}\|_{0,\Omega} + m_2\|\mathbf{z}_{\mathbf{u}}\|_{1,\Omega})\|(\mathbf{x}_{\mathbf{u}}, \mathbf{x}_{\omega})\|_X,$$

where m_1 and m_2 are given by

$$m_1 = \bar{\alpha}^{-1} \max\{2\nu_1, \kappa_1, 2C_r d^{\frac{r-2}{2r}}\|\nabla\nu\|_{0,r^*,\Omega}\}, \quad m_2 = \bar{\alpha}^{-1} \max\{\sigma_1, \nu_1, \kappa_1, \kappa_2, 2C_r d^{\frac{r-2}{2r}}\|\nabla\nu\|_{0,r^*,\Omega}\}.$$

On the other hand, from (3.4) we have

$$\begin{aligned}
a((e_{\mathbf{u}}, e_{\omega}), (\mathbf{x}_{\mathbf{u}}, \mathbf{x}_{\omega})) &= -N(\mathbf{u}; \mathbf{u}, \mathbf{x}_{\mathbf{u}}) + N(\mathbf{u}_h; \mathbf{u}_h, \mathbf{x}_{\mathbf{u}}) - b((\mathbf{x}_{\mathbf{u}}, \mathbf{x}_{\omega}), e_p) \\
&= -N(\mathbf{u}; \mathbf{z}_{\mathbf{u}}, \mathbf{x}_{\mathbf{u}}) - N(\mathbf{u}; \mathbf{x}_{\mathbf{u}}, \mathbf{x}_{\mathbf{u}}) - N(\mathbf{z}_{\mathbf{u}}; \mathbf{u}_h, \mathbf{x}_{\mathbf{u}}) \\
& \quad - N(\mathbf{x}_{\mathbf{u}}; \mathbf{u}_h, \mathbf{x}_{\mathbf{u}}) + (z_p, \operatorname{div} \mathbf{x}_{\mathbf{u}})_{0,\Omega} + (x_p, \operatorname{div} \mathbf{x}_{\mathbf{u}})_{0,\Omega} \\
&\leq C_4^2 d^{1/2}(\|\mathbf{u}\|_{1,\Omega}\|\mathbf{z}_{\mathbf{u}}\|_{1,\Omega}\|\mathbf{x}_{\mathbf{u}}\|_{1,\Omega} + \|\mathbf{u}\|_{1,\Omega}\|\mathbf{x}_{\mathbf{u}}\|_{1,\Omega}^2 + \|\mathbf{u}_h\|_{1,\Omega}\|\mathbf{z}_{\mathbf{u}}\|_{1,\Omega}\|\mathbf{x}_{\mathbf{u}}\|_{1,\Omega} \\
& \quad + \|\mathbf{u}_h\|_{1,\Omega}\|\mathbf{x}_{\mathbf{u}}\|_{1,\Omega}^2) + \|z_p\|_{0,\Omega}\|\operatorname{div} \mathbf{x}_{\mathbf{u}}\|_{0,\Omega} - (x_p, \operatorname{div} \mathbf{v}_h)_{0,\Omega} \\
&\leq (2C_4^2 d^{1/2}\delta\|\mathbf{z}_{\mathbf{u}}\|_{1,\Omega} + \|z_p\|_{0,\Omega})\|(\mathbf{x}_{\mathbf{u}}, \mathbf{x}_{\omega})\|_X + 2C_4^2 d^{1/2}\delta\|(\mathbf{x}_{\mathbf{u}}, \mathbf{x}_{\omega})\|_X^2 - (x_p, \operatorname{div} \mathbf{v}_h)_{0,\Omega},
\end{aligned}$$

where we have used Cauchy-Schwarz inequality. From the above inequality, we obtain

$$\left(1 - \frac{2C_4^2 d^{1/2}\delta}{\bar{\alpha}}\right)\|(\mathbf{x}_{\mathbf{u}}, \mathbf{x}_{\omega})\|_X \leq \left(m_2 + \frac{2C_4^2 d^{1/2}\delta}{\bar{\alpha}}\right)\|\mathbf{z}_{\mathbf{u}}\|_{1,\Omega} + m_1\|\mathbf{z}_{\omega}\|_{0,\Omega} + \bar{\alpha}^{-1}\|z_p\|_{0,\Omega} - \bar{\alpha}^{-1}(x_p, \operatorname{div} \mathbf{v}_h)_{0,\Omega},$$

while by the hypothesis of our problem is easy to see that $1 - \frac{2C_4^2 d^{1/2}\delta}{\bar{\alpha}} > 0$. Therefore,

$$\|(\mathbf{x}_{\mathbf{u}}, \mathbf{x}_{\omega})\|_X \leq M_2\|\mathbf{z}_{\mathbf{u}}\|_{1,\Omega} + M_1\|\mathbf{z}_{\omega}\|_{0,\Omega} + M_3\|z_p\|_{0,\Omega} - M_3(x_p, \operatorname{div} \mathbf{v}_h)_{0,\Omega}, \quad (3.5)$$

where the constants are given by

$$M_2 = \left(1 - \frac{2C_4^2 d^{1/2} \delta}{\bar{\alpha}}\right)^{-1} \left(m_2 + \frac{2C_4^2 d^{1/2} \delta}{\bar{\alpha}}\right), \quad M_1 = m_1 \left(1 - \frac{2C_4^2 d^{1/2} \delta}{\bar{\alpha}}\right)^{-1}, \quad M_3 = \bar{\alpha}^{-1} \left(1 - \frac{2C_4^2 d^{1/2} \delta}{\bar{\alpha}}\right).$$

Next, after introducing the following subspace of V_h :

$$Z_h := \{\mathbf{v}_h \in V_h : (q_h, \operatorname{div} \mathbf{v}_h)_{0,\Omega} = 0, \quad \forall q_h \in Q_h\},$$

we can deduce from (3.5) that

$$\|(\mathbf{u}_h - \mathbf{z}_h, \mathbf{x}_\omega)\|_X \leq M_2 \|\mathbf{u} - \mathbf{z}_h\|_{1,\Omega} + M_1 \|\mathbf{z}_\omega\|_{0,\Omega} + M_3 \|z_p\|_{0,\Omega} \quad \forall \mathbf{z}_h \in Z_h.$$

As V_h and Q_h are stable for the Stokes problem, then, using [41, Proposition 7.4.1] we have that $V_h = Z_h \oplus (Z_h)^\perp$ and there exists $\gamma_1 > 0$ such that

$$\gamma_1 \|\mathbf{o}_h\|_{1,\Omega} \leq \sup_{q_h \in Q_h} \frac{(q_h, \operatorname{div} \mathbf{o}_h)_{0,\Omega}}{\|q_h\|_{0,\Omega}} \quad \forall \mathbf{o}_h \in (Z_h)^\perp. \quad (3.6)$$

From the above, we deduce that for \mathbf{v}_h , there exist $\mathbf{z}_h \in Z_h$ and $\mathbf{o}_h \in (Z_h)^\perp$ such that $\mathbf{v}_h = \mathbf{z}_h + \mathbf{o}_h$. By the triangle inequality, we find

$$\begin{aligned} \|\mathbf{u}_h - \mathbf{v}_h\|_{1,\Omega} &\leq \|\mathbf{u}_h - \mathbf{z}_h\|_{1,\Omega} + \|\mathbf{o}_h\|_{1,\Omega} \\ &\leq \|\mathbf{u}_h - \mathbf{z}_h\|_{1,\Omega} + \gamma_1^{-1} \sup_{q_h \in Q_h} \frac{(q_h, \operatorname{div}(-\mathbf{u} + \mathbf{z}_h + \mathbf{o}_h))_{0,\Omega}}{\|q_h\|_{0,\Omega}} \\ &\leq \|\mathbf{u}_h - \mathbf{z}_h\|_{1,\Omega} + \gamma_1^{-1} \|\operatorname{div}(-\mathbf{u} + \mathbf{v}_h)\|_{0,\Omega} \\ &\leq \|\mathbf{u}_h - \mathbf{z}_h\|_{1,\Omega} + \gamma_1^{-1} \|\mathbf{u} - \mathbf{v}_h\|_{1,\Omega}, \end{aligned}$$

and so

$$\|\mathbf{x}_\mathbf{u}\|_{1,\Omega} \leq \|\mathbf{u}_h - \mathbf{z}_h\|_{1,\Omega} + \gamma_1^{-1} \|\mathbf{z}_\mathbf{u}\|_{1,\Omega}.$$

Then, after algebraic manipulations and using (3.6), we have

$$\begin{aligned} \|(\mathbf{x}_\mathbf{u}, \mathbf{x}_\omega)\|_X &\leq \|\mathbf{x}_\mathbf{u}\|_{1,\Omega} + \|\mathbf{x}_\omega\|_{0,\Omega} \leq \|\mathbf{u}_h - \mathbf{z}_h\|_{1,\Omega} + \gamma_1^{-1} \|\mathbf{z}_\mathbf{u}\|_{1,\Omega} + \|\mathbf{x}_\omega\|_{0,\Omega} \\ &\leq \sqrt{2}(\|\mathbf{u}_h - \mathbf{z}_h\|_{1,\Omega}^2 + \|\mathbf{x}_\omega\|_{0,\Omega}^2)^{1/2} + \gamma_1^{-1} \|\mathbf{z}_\mathbf{u}\|_{1,\Omega} \\ &= \sqrt{2} \|(\mathbf{u}_h - \mathbf{z}_h, \mathbf{x}_\omega)\|_X + \gamma_1^{-1} \|\mathbf{z}_\mathbf{u}\|_{1,\Omega} \\ &\leq \sqrt{2}(M_2 \|\mathbf{u} - \mathbf{z}_h\|_{1,\Omega} + M_1 \|\mathbf{z}_\omega\|_{0,\Omega} + M_3 \|z_p\|_{0,\Omega}) + \gamma_1^{-1} \|\mathbf{z}_\mathbf{u}\|_{1,\Omega}, \\ &\leq \sqrt{2}(M_2(\|\mathbf{u} - \mathbf{v}_h\|_{1,\Omega} + \|\mathbf{o}_h\|_{1,\Omega}) + M_1 \|\mathbf{z}_\omega\|_{0,\Omega} + M_3 \|z_p\|_{0,\Omega}) + \gamma_1^{-1} \|\mathbf{z}_\mathbf{u}\|_{1,\Omega}, \\ &\leq \sqrt{2}(M_2(\|\mathbf{z}_\mathbf{u}\|_{1,\Omega} + \gamma_1^{-1} \|\mathbf{z}_\mathbf{u}\|_{1,\Omega}) + M_1 \|\mathbf{z}_\omega\|_{0,\Omega} + M_3 \|z_p\|_{0,\Omega}) + \gamma_1^{-1} \|\mathbf{z}_\mathbf{u}\|_{1,\Omega}, \\ &\leq (\sqrt{2}M_2 + \gamma_1^{-1}(1 + \sqrt{2})) \|\mathbf{z}_\mathbf{u}\|_{1,\Omega} + \sqrt{2}M_1 \|\mathbf{z}_\omega\|_{0,\Omega} + \sqrt{2}M_3 \|z_p\|_{0,\Omega}. \end{aligned}$$

On the other hand, from (3.1) and (3.4), we can assert that

$$\begin{aligned} \|x_p\|_{0,\Omega} &\leq \gamma_0^{-1} \sup_{(\mathbf{v}_h, \boldsymbol{\theta}_h) \in V_h \times W_h} \frac{b((\mathbf{v}_h, \boldsymbol{\theta}_h), x_p)}{\|(\mathbf{v}_h, \boldsymbol{\theta}_h)\|_X} \\ &= \gamma_0^{-1} \sup_{(\mathbf{v}_h, \boldsymbol{\theta}_h) \in V_h \times W_h} \frac{-a((e_\mathbf{u}, e_\omega), (\mathbf{v}_h, \boldsymbol{\theta}_h)) - N(\mathbf{u}; \mathbf{u}, \mathbf{v}_h) + N(\mathbf{u}_h; \mathbf{u}_h, \mathbf{v}_h) - b((\mathbf{v}_h, \boldsymbol{\theta}_h), z_p)}{\|(\mathbf{v}_h, \boldsymbol{\theta}_h)\|_X} \\ &= \gamma_0^{-1} \sup_{(\mathbf{v}_h, \boldsymbol{\theta}_h) \in V_h \times W_h} \frac{-a((e_\mathbf{u}, e_\omega), (\mathbf{v}_h, \boldsymbol{\theta}_h)) - N(\mathbf{u}; e_\mathbf{u}, \mathbf{v}_h) - N(e_\mathbf{u}; \mathbf{u}_h, \mathbf{v}_h) - b((\mathbf{v}_h, \boldsymbol{\theta}_h), z_p)}{\|(\mathbf{v}_h, \boldsymbol{\theta}_h)\|_X} \\ &\leq \gamma_0^{-1} (\|a\| + 2C_4^2 d^{1/2} \delta) \|(e_\mathbf{u}, e_\omega)\|_X + \gamma_0^{-1} \|z_p\|_{0,\Omega}. \end{aligned}$$

Therefore, we end up with the bounds

$$\begin{aligned}
\|(e_{\mathbf{u}}, e_{\boldsymbol{\omega}}, e_p)\|_H &\leq \|(\mathbf{z}_{\mathbf{u}}, \mathbf{z}_{\boldsymbol{\omega}}, z_p)\|_H + \|(\mathbf{x}_{\mathbf{u}}, \mathbf{x}_{\boldsymbol{\omega}}, x_p)\|_H \leq \|(\mathbf{z}_{\mathbf{u}}, \mathbf{z}_{\boldsymbol{\omega}}, z_p)\|_H + \|(\mathbf{x}_{\mathbf{u}}, \mathbf{x}_{\boldsymbol{\omega}})\|_X + \|x_p\|_{0,\Omega} \\
&\leq \|(\mathbf{z}_{\mathbf{u}}, \mathbf{z}_{\boldsymbol{\omega}}, z_p)\|_H + \widehat{M}_2 \|\mathbf{z}_{\mathbf{u}}\|_{1,\Omega} + \widehat{M}_1 \|\mathbf{z}_{\boldsymbol{\omega}}\|_{0,\Omega} + \widehat{M}_3 \|z_p\|_{0,\Omega} \\
&\quad + \gamma_0^{-1} (\|a\| + 2C_4^2 d^{1/2} \delta) \| (e_{\mathbf{u}}, e_{\boldsymbol{\omega}}) \|_X + \gamma_0^{-1} \|z_p\|_{0,\Omega} \\
&\leq \|(\mathbf{z}_{\mathbf{u}}, \mathbf{z}_{\boldsymbol{\omega}}, z_p)\|_H + \widehat{M}_2 \|\mathbf{z}_{\mathbf{u}}\|_{1,\Omega} + \widehat{M}_1 \|\mathbf{z}_{\boldsymbol{\omega}}\|_{0,\Omega} + \widehat{M}_3 \|z_p\|_{0,\Omega} \\
&\quad + \gamma_0^{-1} (\|a\| + 2C_4^2 d^{1/2} \delta) (\|(\mathbf{z}_{\mathbf{u}}, \mathbf{z}_{\boldsymbol{\omega}})\|_X + \|(\mathbf{x}_{\mathbf{u}}, \mathbf{x}_{\boldsymbol{\omega}})\|_X) + \gamma_0^{-1} \|z_p\|_{0,\Omega} \\
&\leq \|(\mathbf{z}_{\mathbf{u}}, \mathbf{z}_{\boldsymbol{\omega}}, z_p)\|_H + \widehat{M}_2 \|\mathbf{z}_{\mathbf{u}}\|_{1,\Omega} + \widehat{M}_1 \|\mathbf{z}_{\boldsymbol{\omega}}\|_{0,\Omega} + \widehat{M}_3 \|z_p\|_{0,\Omega} + \gamma_0^{-1} \|z_p\|_{0,\Omega} \\
&\quad + \widehat{M}_4 \|(\mathbf{z}_{\mathbf{u}}, \mathbf{z}_{\boldsymbol{\omega}})\|_X + \widehat{M}_4 \widehat{M}_2 \|\mathbf{z}_{\mathbf{u}}\|_{1,\Omega} + \widehat{M}_4 \widehat{M}_1 \|\mathbf{z}_{\boldsymbol{\omega}}\|_{0,\Omega} + \widehat{M}_4 \widehat{M}_3 \|z_p\|_{0,\Omega}.
\end{aligned}$$

And consequently, we obtain the estimate

$$\|(e_{\mathbf{u}}, e_{\boldsymbol{\omega}}, e_p)\|_H \leq (1 + \widehat{M}_4)(1 + \widehat{M}_1 + \widehat{M}_2) \|(\mathbf{z}_{\mathbf{u}}, \mathbf{z}_{\boldsymbol{\omega}})\|_X + \widehat{M}_5 \|z_p\|_{0,\Omega},$$

where the involved constants are

$$\begin{aligned}
\widehat{M}_1 &= \sqrt{2}M_1, \quad \widehat{M}_2 = \sqrt{2}M_2 + \gamma_1^{-1}(1 + \sqrt{2}), \quad \widehat{M}_3 = \sqrt{2}M_3, \\
\widehat{M}_4 &= \gamma_0^{-1} (\|a\| + 2C_4^2 d^{1/2} \delta), \quad \widehat{M}_5 = 1 + \gamma_0^{-1} + (1 + \widehat{M}_4) \widehat{M}_3.
\end{aligned}$$

□

3.3. Discrete subspaces and error estimates

In this section we give examples of finite element spaces for V_h, Q_h, W_h and derive the corresponding rate of convergence for each finite element family.

Generalised Taylor–Hood– \mathbb{P}_k . We begin with Taylor–Hood finite elements [35] to approximate velocity and pressure, and we will contemplate continuous or discontinuous piecewise polynomial spaces for vorticity. More precisely, for any $k \geq 1$, we consider

$$\begin{aligned}
V_h &:= \{\mathbf{v}_h \in C(\overline{\Omega})^d : \mathbf{v}_h|_K \in \mathbb{P}_{k+1}(K)^d \quad \forall K \in \mathcal{T}_h\} \cap \mathbf{H}_0^1(\Omega)^d, \\
Q_h &:= \{q_h \in C(\overline{\Omega}) : q_h|_K \in \mathbb{P}_k(K) \quad \forall K \in \mathcal{T}_h\} \cap L_0^2(\Omega), \\
W_h^1 &:= \{\boldsymbol{\theta}_h \in C(\overline{\Omega})^{d(d-1)/2} : \boldsymbol{\theta}_h|_K \in \mathbb{P}_k(K)^{d(d-1)/2} \quad \forall K \in \mathcal{T}_h\}, \\
W_h^2 &:= \{\boldsymbol{\theta}_h \in L^2(\Omega)^{d(d-1)/2} : \boldsymbol{\theta}_h|_K \in \mathbb{P}_k(K)^{d(d-1)/2} \quad \forall K \in \mathcal{T}_h\}.
\end{aligned} \tag{3.7}$$

It is well known that (V_h, Q_h) satisfies the inf-sup condition (3.1) (see [33]). Let us recall approximation properties of the finite element subspaces (3.7). Assume that $\mathbf{u} \in H^{1+s}(\Omega)^d$, $p \in H^s(\Omega)$ and $\boldsymbol{\omega} \in H^s(\Omega)^{d(d-1)/2}$, for some $s \in (1/2, k+1]$. Then there exists $C > 0$, independent of h , such that

$$\inf_{\mathbf{v}_h \in V_h} \|\mathbf{u} - \mathbf{v}_h\|_{1,\Omega} \leq Ch^s \|\mathbf{u}\|_{1+s,\Omega}, \quad \inf_{q_h \in Q_h} \|p - q_h\|_{0,\Omega} \leq Ch^s \|p\|_{s,\Omega}, \tag{3.8a}$$

$$\inf_{\boldsymbol{\theta}_h \in W_h^1} \|\boldsymbol{\omega} - \boldsymbol{\theta}_h\|_{0,\Omega} \leq Ch^s \|\boldsymbol{\omega}\|_{s,\Omega}, \quad \inf_{\boldsymbol{\theta}_h \in W_h^2} \|\boldsymbol{\omega} - \boldsymbol{\theta}_h\|_{0,\Omega} \leq Ch^s \|\boldsymbol{\omega}\|_{s,\Omega}. \tag{3.8b}$$

The following theorem provides the rate of convergence expected when using (3.2). The proof follows directly from Theorem 3.2 in combination with (3.8a)–(3.8b).

Theorem 3.3. *Let $k \geq 1$ be a integer and let V_h, Q_h and W_h^i , $i = 1, 2$ be given by (3.7). Let $(\mathbf{u}, \boldsymbol{\omega}, p) \in \mathbf{H}_0^1(\Omega)^d \times L^2(\Omega)^{d(d-1)/2} \times L_0^2(\Omega)$ and $(\mathbf{u}_h, \boldsymbol{\omega}_h, p_h) \in V_h \times W_h^i \times Q_h$ be the unique solutions to the continuous and discrete problems (1.2) and (3.2), respectively. Assume that $\mathbf{u} \in H^{1+s}(\Omega)^d$, $\boldsymbol{\omega} \in H^s(\Omega)^{d(d-1)/2}$ and $p \in H^s(\Omega)$, for some $s \in (1/2, k+1]$. Then, there exists $\hat{C} > 0$, independent of h , such that*

$$\|(\mathbf{u}, \boldsymbol{\omega}) - (\mathbf{u}_h, \boldsymbol{\omega}_h)\|_X + \|p - p_h\|_{0,\Omega} \leq \hat{C}h^s (\|\mathbf{u}\|_{1+s,\Omega} + \|\boldsymbol{\omega}\|_{s,\Omega} + \|p\|_{s,\Omega}).$$

MINI-element- \mathbb{P}_k . The second family of finite element is based on the so-called MINI-element for velocity and pressure [14], and continuous or discontinuous piecewise polynomials for vorticity (see [22, Sections 8.6 and 8.7] for further details):

$$\begin{aligned} H_h &:= \{\mathbf{v}_h \in C(\bar{\Omega})^d : \mathbf{v}_h|_K \in \mathbb{P}_k(K)^d \quad \forall K \in \mathcal{T}_h\}, \quad U_h := H_h^d, \\ \mathbb{B}(b_K \nabla H_h) &:= \{\mathbf{v}_{hb} \in H^1(\Omega)^d : \mathbf{v}_{hb}|_K = b_K \nabla(q_h)|_K \text{ for some } q_h \in H_h\}, \end{aligned}$$

where b_K is the standard (cubic or quartic) bubble function $\lambda_1 \cdots \lambda_{d+1} \in \mathbb{P}_{d+1}(K)$, and let us define the following finite element subspaces:

$$\begin{aligned} Q_h &:= \{q_h \in C(\bar{\Omega}) : q_h|_K \in \mathbb{P}_k(K) \quad \forall K \in \mathcal{T}_h\} \cap L_0^2(\Omega), \quad V_h := U_h \oplus \mathbb{B}(b_K \nabla Q_h) \cap H_0^1(\Omega)^d, \\ W_h^1 &:= \{\boldsymbol{\theta}_h \in C(\bar{\Omega})^{d(d-1)/2} : \boldsymbol{\theta}_h|_K \in \mathbb{P}_k(K)^{d(d-1)/2} \quad \forall K \in \mathcal{T}_h\}, \\ W_h^2 &:= \{\boldsymbol{\theta}_h \in L^2(\Omega)^{d(d-1)/2} : \boldsymbol{\theta}_h|_K \in \mathbb{P}_k(K)^{d(d-1)/2} \quad \forall K \in \mathcal{T}_h\}. \end{aligned} \quad (3.9)$$

The rate of convergence considering the above discrete spaces (3.9) is obtained similarly as before, from the Céa estimate and the approximation properties.

Theorem 3.4. *Let $k \geq 1$ be a integer and let V_h, Q_h and W_h^i , $i = 1, 2$ be given by (3.9). Let $(\mathbf{u}, \boldsymbol{\omega}, p) \in H_0^1(\Omega)^d \times L^2(\Omega)^{d(d-1)/2} \times L_0^2(\Omega)$ and $(\mathbf{u}_h, \boldsymbol{\omega}_h, p_h) \in V_h \times W_h^i \times Q_h$ be the unique solutions to the continuous and discrete problems (1.2) and (3.2), respectively. Assume that $\mathbf{u} \in H^{1+s}(\Omega)^d$, $\boldsymbol{\omega} \in H^s(\Omega)^{d(d-1)/2}$ and $p \in H^s(\Omega)$, for some $s \in (1/2, k]$. Then, there exists $\hat{C} > 0$, independent of h , such that*

$$\|(\mathbf{u}, \boldsymbol{\omega}) - (\mathbf{u}_h, \boldsymbol{\omega}_h)\|_X + \|p - p_h\|_{0,\Omega} \leq \hat{C} h^s (\|\mathbf{u}\|_{1+s,\Omega} + \|\boldsymbol{\omega}\|_{s,\Omega} + \|p\|_{s,\Omega}).$$

Bernardi–Raugel- \mathbb{P}_k . Finally we specify a family of finite elements based on the Bernardi–Raugel element for velocity and pressure [19], and continuous or discontinuous piecewise linear polynomials for vorticity. Let us introduce the following local space of order k

$$\mathbb{P}_{1\mathbf{n}}(K)^d := \mathbb{P}_1(K)^d \oplus \text{span}\{\mathbf{w}_1, \mathbf{w}_2, \mathbf{w}_3, \mathbf{w}_4\},$$

with the vector-valued functions $\mathbf{w}_i := \lambda_j \lambda_k \lambda_l \mathbf{n}_i \in \mathbb{P}_3(K)^d$, $j, k, l \neq i$, $j, k \neq l$, $j \neq k$, with \mathbf{n}_i the outer normal to the face i . Using the subspaces

$$\begin{aligned} V_h &:= \{\mathbf{v}_h \in C(\bar{\Omega})^d : \mathbf{v}_h|_K \in \mathbb{P}_{1\mathbf{n}}(K)^d \quad \forall K \in \mathcal{T}_h\} \cap H_0^1(\Omega)^d, \\ Q_h &:= \{q_h \in L^2(\Omega) : q_h|_K \in \mathbb{P}_0(K) \quad \forall K \in \mathcal{T}_h\} \cap L_0^2(\Omega), \\ W_h^1 &:= \{\boldsymbol{\theta}_h \in C(\bar{\Omega})^{d(d-1)/2} : \boldsymbol{\theta}_h|_K \in \mathbb{P}_1(K)^{d(d-1)/2} \quad \forall K \in \mathcal{T}_h\}, \\ W_h^2 &:= \{\boldsymbol{\theta}_h \in L^2(\Omega)^{d(d-1)/2} : \boldsymbol{\theta}_h|_K \in \mathbb{P}_0(K)^{d(d-1)/2} \quad \forall K \in \mathcal{T}_h\}, \end{aligned} \quad (3.10)$$

the rate of convergence of the augmented mixed finite element scheme is as follows:

Theorem 3.5. *Let V_h, Q_h and W_h^i , $i = 1, 2$ be given by (3.10). Let $(\mathbf{u}, \boldsymbol{\omega}, p) \in H_0^1(\Omega)^d \times L^2(\Omega)^{d(d-1)/2} \times L_0^2(\Omega)$ and $(\mathbf{u}_h, \boldsymbol{\omega}_h, p_h) \in V_h \times W_h^i \times Q_h$ be the unique solutions to the continuous and discrete problems (1.2) and (3.2), respectively. Assume that $\mathbf{u} \in H^{1+s}(\Omega)^d$, $\boldsymbol{\omega} \in H^s(\Omega)^{d(d-1)/2}$ and $p \in H^s(\Omega)$, for some $s \in (1/2, 1]$. Then, there exists $\hat{C} > 0$, independent of h , such that*

$$\|(\mathbf{u}, \boldsymbol{\omega}) - (\mathbf{u}_h, \boldsymbol{\omega}_h)\|_X + \|p - p_h\|_{0,\Omega} \leq \hat{C} h^s (\|\mathbf{u}\|_{1+s,\Omega} + \|\boldsymbol{\omega}\|_{s,\Omega} + \|p\|_{s,\Omega}).$$

4. NUMERICAL RESULTS

In this section, we present some numerical experiments that serve to verify numerically the convergence rates predicted by Theorems 3.3, 3.4, and that illustrate the performance of the proposed methods in typical incompressible flow problems. We implement the finite element routines using the libraries FEniCS [3] and FreeFem++ [34]. The nonlinear systems are solved with a Newton-Raphson method with zero initial guess, and prescribing a tolerance of 10^{-8} on the either absolute or relative ℓ^∞ norm of the residuals. Unless otherwise specified, all linear solves performed at each nonlinear iteration step are conducted with the direct solver MUMPS [6].

TABLE 4.1. Example 1A: Accuracy verification in 2D for different finite element families for the approximation of velocity and pressure, whereas for the vorticity, discontinuous \mathbb{P}_1 elements (the space W_h^2) are used in all cases.

DoF	h	$\ \mathbf{u} - \mathbf{u}_h\ _{1,\Omega}$	$r(\mathbf{u})$	$\ \boldsymbol{\omega} - \boldsymbol{\omega}_h\ _{0,\Omega}$	$r(\boldsymbol{\omega})$	$\ p - p_h\ _{0,\Omega}$	$r(p)$
Taylor–Hood element							
84	0.707	8.52e-01	–	5.44e-01	–	2.33e-01	–
284	0.354	2.49e-01	1.772	1.41e-01	1.948	4.64e-02	2.326
1044	0.177	5.78e-02	2.110	3.35e-02	2.073	7.38e-03	2.651
4004	0.088	1.29e-02	2.163	8.21e-03	2.028	1.67e-03	2.148
15684	0.044	3.05e-03	2.081	2.04e-03	2.008	4.06e-04	2.038
62084	0.022	7.50e-04	2.024	5.09e-04	2.003	1.01e-04	2.010
247044	0.011	1.87e-04	2.006	1.27e-04	2.001	2.51e-05	2.003
MINI-element							
68	0.707	2.58e+0	–	1.05e+0	–	4.26e-01	–
236	0.354	1.53e+0	0.760	4.40e-01	1.261	9.12e-02	2.224
884	0.177	7.69e-01	0.988	2.16e-01	1.024	2.30e-02	1.989
3428	0.088	3.83e-01	1.007	1.07e-01	1.020	5.71e-03	2.009
13508	0.044	1.91e-01	1.003	5.30e-02	1.008	1.51e-03	1.917
53636	0.022	9.55e-02	1.001	2.65e-02	1.002	4.19e-04	1.851
213764	0.011	4.77e-02	1.000	1.32e-02	1.000	1.22e-04	1.777
Bernardi–Raugel element							
66	0.707	1.07e+0	–	8.26e-01	–	2.79e-01	–
234	0.354	5.14e-01	1.067	3.46e-01	1.252	1.50e-01	0.892
882	0.177	2.70e-01	0.928	1.81e-01	0.931	7.15e-02	1.075
3426	0.088	1.40e-01	0.947	9.58e-02	0.924	3.41e-02	1.066
13506	0.044	7.08e-02	0.984	4.86e-02	0.977	1.67e-02	1.026
53634	0.022	3.55e-02	0.995	2.44e-02	0.992	8.33e-03	1.008
213762	0.011	1.77e-02	0.998	1.22e-02	0.997	4.16e-03	1.002
Crouzeix-Raviart element							
65	0.707	2.33e+0	–	1.92e+0	–	4.39e-01	–
241	0.354	2.19e+0	0.084	1.14e+0	0.754	4.02e-01	0.126
929	0.177	1.38e+0	0.748	5.47e-01	1.057	2.25e-01	0.962
3649	0.088	6.60e-01	1.069	2.35e-01	1.218	9.02e-02	1.321
14465	0.044	3.21e-01	1.038	1.10e-01	1.091	4.12e-02	1.131
57601	0.022	1.58e-01	1.024	5.42e-02	1.026	2.00e-02	1.039
229889	0.011	7.82e-02	1.014	2.69e-02	1.007	9.95e-03	1.010

4.1. Example 1: Convergence tests in 2D and 3D

To numerically investigate the accuracy of the proposed finite element formulation, we consider the unit square and unit cube domains $\Omega = (0, 1)^2$, $\Omega = (0, 1)^3$ discretised into uniform triangular/tetrahedral elements. Sequences of successively refined meshes are constructed and the numerical solutions obtained on each refinement level are compared against manufactured exact solutions in the 2D and 3D cases, defined respectively as

$$\mathbf{u}(x, y) = \begin{pmatrix} \cos(\pi x) \sin(\pi y) \\ -\sin(\pi x) \cos(\pi y) \end{pmatrix}, \quad \mathbf{u}(x, y, z) = \begin{pmatrix} \sin(\pi x) \cos(\pi y) \cos(\pi z) \\ -2 \cos(\pi x) \sin(\pi y) \cos(\pi z) \\ \cos(\pi x) \cos(\pi y) \sin(\pi z) \end{pmatrix},$$

$$p(x, y) = \sin(\pi x) \sin(\pi y), \quad p(x, y, z) = 1 - \cos(xyz) \sin(xyz),$$

TABLE 4.2. Example 1B: Error profiles and experimental rates of convergence for velocity, vorticity, and pressure approximation in 3D generated with different finite element families.

DoF	h	$\ \mathbf{u} - \mathbf{u}_h\ _{1,\Omega}$	$r(\mathbf{u})$	$\ \boldsymbol{\omega} - \boldsymbol{\omega}_h\ _{0,\Omega}$	$r(\boldsymbol{\omega})$	$\ p - p_h\ _{0,\Omega}$	$r(p)$
Taylor–Hood and $\mathbb{P}_1 (W_h^1)$							
484	0.866	1.43e+0	–	1.14e+0	–	1.28e-01	–
2688	0.433	3.78e-01	1.925	3.20e-01	1.833	1.41e-02	3.189
17656	0.217	9.57e-02	1.982	6.85e-02	2.223	1.61e-03	3.130
127464	0.108	2.32e-02	2.047	1.62e-02	2.080	2.26e-04	2.834
967624	0.054	5.60e-03	1.929	3.99e-03	2.095	5.36e-05	2.387
MINI-element and $\mathbb{P}_1 (W_h^1)$							
334	0.866	5.29e+0	–	1.78e+0	–	7.75e-01	–
2028	0.433	2.93e+0	0.852	7.23e-01	1.301	4.18e-01	0.890
14320	0.217	1.29e+0	1.189	2.22e-01	1.703	1.10e-01	1.926
108120	0.108	6.05e-01	1.089	6.45e-02	1.785	2.93e-02	1.910
841384	0.054	2.96e-01	1.031	1.90e-02	1.765	8.21e-03	1.835
Crouzeix-Raviart and $\mathbb{P}_0 (W_h^2$ with $k = 0)$							
553	0.866	2.84e-01	–	1.92e-01	–	7.72e-02	–
4129	0.433	1.39e-01	1.028	7.59e-02	1.343	3.62e-02	1.094
31873	0.217	4.58e-02	1.602	2.48e-02	1.616	1.61e-02	1.167
250369	0.108	1.34e-02	1.774	7.96e-03	1.637	7.85e-03	1.036
1984513	0.054	4.33e-03	1.588	2.81e-03	1.609	3.82e-03	1.121

with $\boldsymbol{\omega} = \mathbf{curl} \mathbf{u}$, with permeability $\kappa = 0.1$, with the following distributions of 2D and 3D viscosities

$$\nu(x, y) = \nu_0 + (\nu_1 - \nu_0) \cos(\pi xy) \cos(\pi xy), \quad \nu(x, y, z) = \nu_0 + (\nu_1 - \nu_0) x^2 y^2 z^2,$$

and with $\sigma(\mathbf{x}) = \kappa^{-1} \nu(\mathbf{x})$. The velocities are divergence-free. Moreover, the viscosities are smooth, uniformly bounded, and characterised by the parameters $\nu_0 = 0.1$, $\nu_1 = 1$. The augmentation constants assume the values $\kappa_1 = \frac{2}{3} \nu_0$ and $\kappa_2 = \frac{1}{2} \nu_0$. Since the exact velocity is enforced essentially everywhere on the boundary, the mean value of pressure is to be fixed (to match that of the exact pressure). This is done with a real Lagrange multiplier. Moreover, the source term \mathbf{f} is constructed from the momentum balance equation so that the closed-form solutions above become an exact solution of the problem.

Errors between exact and approximate numerical solutions in the individual norms for velocity, vorticity and pressure are shown with respect to the number of degrees of freedom (DoF) in Tables 4.1 and 4.2 for the 2D and 3D cases, respectively. These errors were produced with the use of Taylor–Hood [35], MINI-element [14], Bernardi–Raugel elements [19], and for sake of illustration, for 2D we include as well the non-conforming Crouzeix–Raviart elements with facet stabilisation [25]. We also tabulate the local experimental rate of error decay for the generic vector or scalar field s , computed as

$$r(s) = \log(\mathbf{e}(s)/\widehat{\mathbf{e}}(s)) [\log(h/\widehat{h})]^{-1},$$

where \mathbf{e} and $\widehat{\mathbf{e}}$ denote errors produced on two consecutive meshes associated with mesh sizes h and \widehat{h} , respectively. In all instances we observe a monotonic optimal convergence, as supported by Theorems 3.3, 3.4, 3.5. For MINI-elements we observe a higher convergence than the one anticipated for pressure. For these tests the number of Newton–Raphson steps required to achieve the prescribed tolerance was, in average, 3. Similar results as those reported herein were obtained by replacing the viscosities described above, with profiles exhibiting higher gradients.

4.2. Example 2: Lid-driven wide cavity flow

Consider now the modified lid-driven cavity benchmark problem in the case of a wide two-dimensional domain $\Omega = (0, 2) \times (0, 1)$. The mesh is structured and with 200×100 vertices. The grid is stretched to cluster towards the

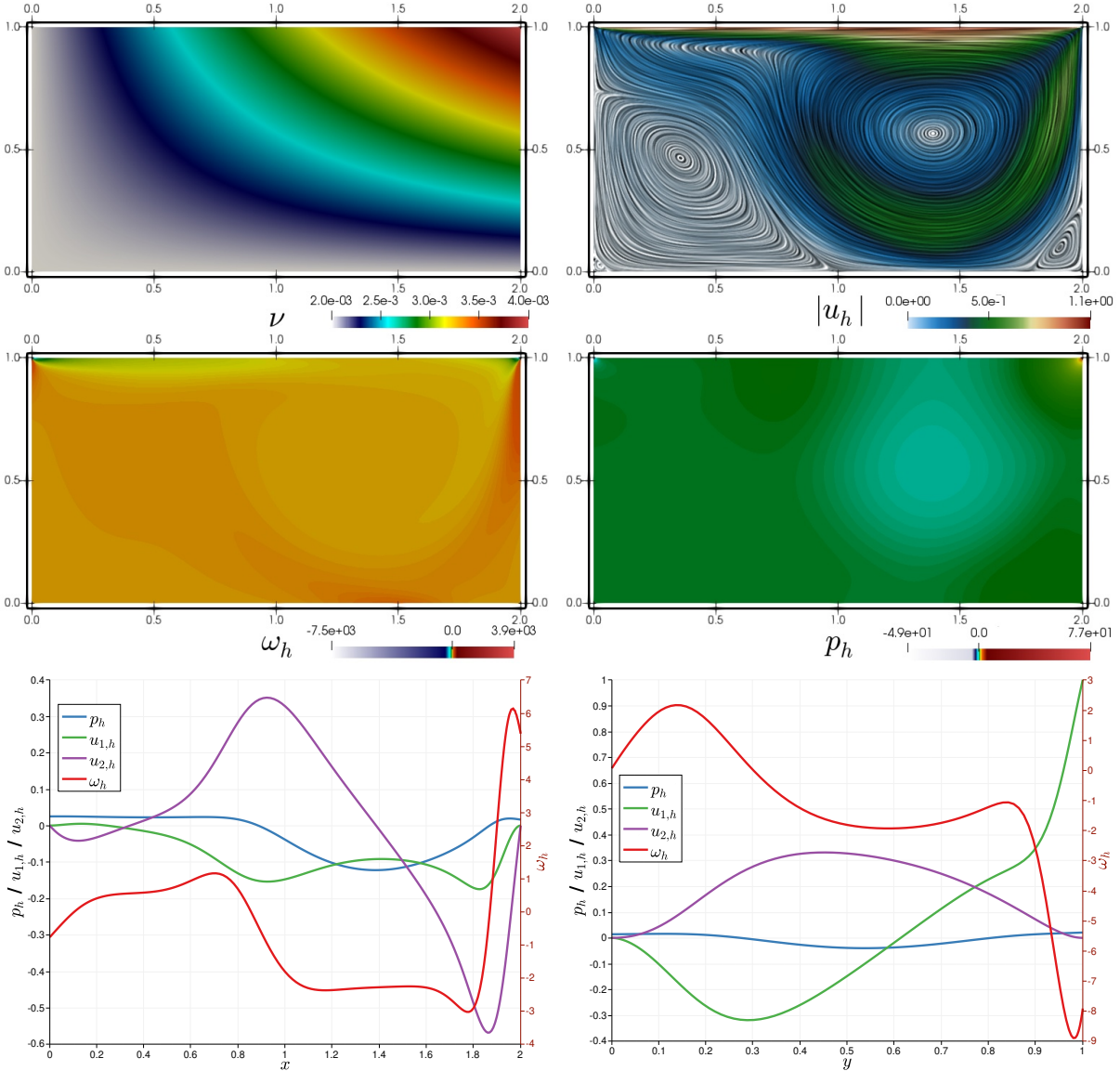


FIGURE 4.1. Example 2: Lid-driven wide cavity. Distribution of variable kinematic viscosity, and portrait of approximate solutions (velocity magnitude with velocity line integral convolution paths, scalar vorticity, and pressure profile). The bottom panels show cuts on the horizontal ($y = 0.5$) and vertical ($x = 1$) midlines of the cavity along with solution profiles.

boundaries. We use in this case the MINI-element plus W_h^1 space for vorticity. The viscosity is $\nu = \nu_0(1 + \frac{1}{2}xy)$ with $\nu_0 = 0.002$, and the external force is zero $\mathbf{f} = \mathbf{0}$. The top wall is moving to the right with constant velocity $\mathbf{u} = (1, 0)^\top$ while the other sub-boundaries are equipped with a no-slip velocity condition, implying that a discontinuity exists in the Dirichlet datum. Again the mean-value of the pressure is fixed (to be zero) with a real Lagrange multiplier. We stress that, even in the case of constant viscosity, the exact solutions for this classical problem are not known. We report the obtained approximate flow patterns in Figure 4.1. The first row shows the imposed viscosity profile (which also defines a variable Brinkman parameter σ), the velocity field with line integral convolution to better visualise the velocity recirculation and vortices (which differs from the usual square lid-driven cavity flow) and indicating well-resolved flow patterns, and the middle row displays scalar vorticity and pressure distributions. The usual corner singularities are seen in the pressure profiles, but no spurious oscillations are observed. We also show in the bottom row plots of the solutions on the midlines $y = 0.5$ and $x = 1$.

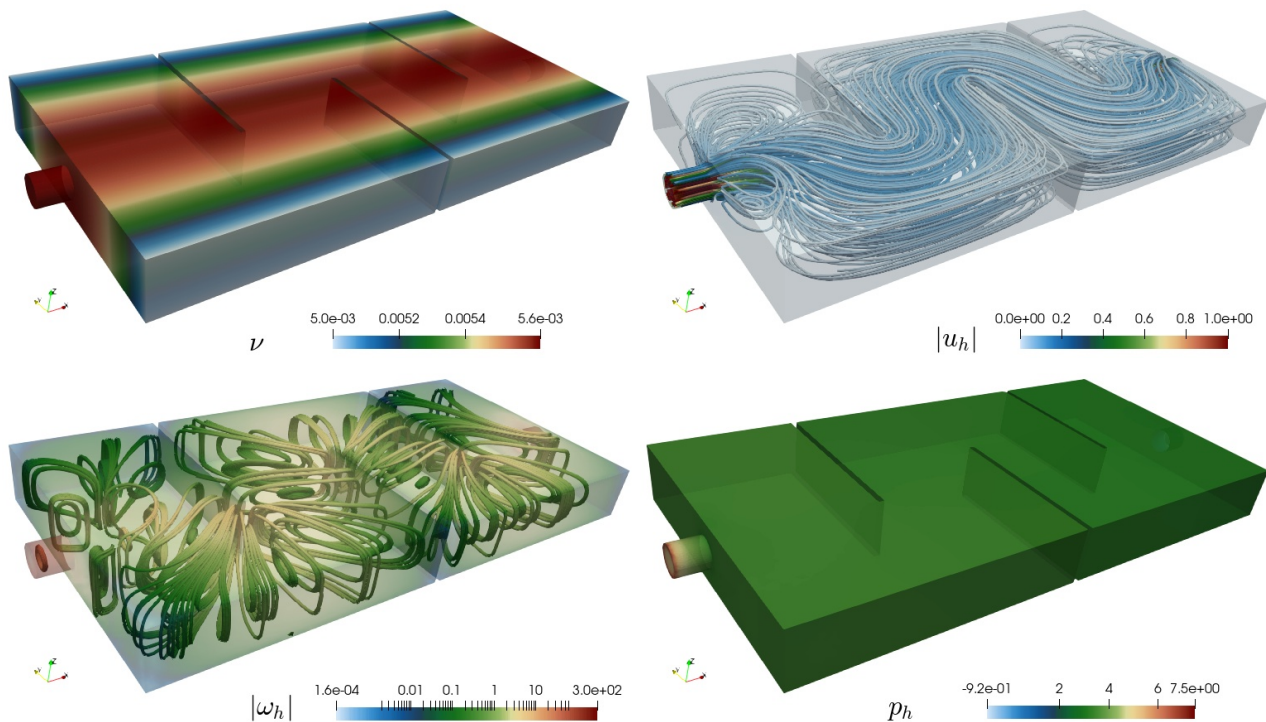


FIGURE 4.2. Example 3: Flow in a maze-shaped geometry. Distribution of variable kinematic viscosity, and portrait of approximate solutions (velocity magnitude and velocity streamlines, vorticity magnitude and vorticity streamlines, and pressure profile).

4.3. Example 3: Flow in a maze-shaped 3D geometry

To conclude the set of numerical examples we present the simulation of three-dimensional flow over obstacles as those encountered in mazes. The geometry and the mesh have been generated using the mesh manipulator Gmsh [32]. The resulting tetrahedral mesh has 193375 elements and 40418 vertices. For this example the viscosity assumes the form $\nu = nu_0(1 + \frac{1}{2}y(1 - y))$ with $\nu_0 = 0.005$. The channel has a length of 2.2 (aligned with the x axis), a width of 1, and a height of 0.2. The boundary of the domain is partitioned into an inflow surface (a disk of radius 0.05 located on the plane x_{\min}), an outflow surface (the disk of the same dimensions, located at x_{\max}), and the remainder of the boundary is constituted by the walls of the maze. On the inflow, a constant inlet velocity is prescribed $\mathbf{u}_{\text{in}} = (1, 0, 0)^{\text{T}}$, no-slip velocities are considered on the walls, and zero pseudo-stress is imposed as outflow boundary condition. These boundary conditions do not coincide with the pure Dirichlet case analysed in the paper. As in the previous example, we consider $\mathbf{f} = \mathbf{0}$. Dictated by inf-sup stability requirements, we use again the MINI-element plus piecewise linear vorticity approximation in W_h^1 .

A graphical illustration regarding the behaviour of the channeling flow is given in Figure 4.2, showing a higher viscosity near the centre of the channel. The velocity streamlines plotted on the top-right panel clearly exemplify the flow patterns commonly found for this regime (with maximal Reynolds number of $\text{Re} = \frac{\text{vel} \cdot \text{diam}}{\nu_0} = \frac{1 \cdot 0.1}{0.005} = 20$), namely a very mild recirculation near the walls adjacent to the inlet and an almost Poiseuille flow, showing higher velocity magnitude towards the centre of the channel. Also, and as expected, the pressure drops from inlet to outlet, and it has the imposed zero mean value.

5. SUMMARY AND CONCLUDING REMARKS

In the present work, we have presented an optimally convergent mixed finite element method for the discretisation of the vorticity-velocity-pressure formulation of the Navier–Stokes equations with non-constant viscosity. We have established the unique solvability of the continuous and discrete variational problems using the theory of fixed-point operators, and have shown the stability and optimal convergence of particular choices of finite element

families. We have numerically investigated the performance of the methods on 2D and 3D tests. Some key features of the proposed method are the liberty to choose different inf-sup stable finite element families for the Navier–Stokes equations, the direct and accurate access to vorticity independently and without applying postprocessing, and the flexibility in handling Dirichlet boundary conditions for velocity, as well as in defining outflow conditions. Some of these properties are of marked interest, for instance, when coupling with other effects such as settling mechanisms or doubly-diffusive interactions, where we foresee a direct applicability of the ideas proposed herein. On the other hand, one unavoidable disadvantage of the present method is that it does not produce point-wise divergence-free velocities.

Acknowledgements. This work has been partially supported by DIUBB through projects 2020127 IF/R and 2120173 GI/C; by ANID-Chile through projects FONDECYT 1211265, FB210005 of the PIA Program: “Concurso Apoyo a Centros Científicos y Tecnológicos de Excelencia con Financiamiento Basal, Scholarship Program, Doctorado Becas Chile 2021”, 21210945; by the Monash Mathematics Research Fund S05802-3951284; and by the Ministry of Science and Higher Education of the Russian Federation within the framework of state support for the creation and development of World-Class Research Centers “Digital biodesign and personalised healthcare” No. 075-15-2020-926.

REFERENCES

- [1] M. ABDELWAHED, E. ALHARBI, N. CHORFI, AND H. OUERTANI, *Resolution and implementation of the nonstationary vorticity velocity pressure formulation of the Navier–Stokes equations*. *Boundary Value Prob.*, 2020 (2020) e167.
- [2] R.A. ADAMS, AND J.J.F. FOURNIER, *Sobolev Spaces*, Second edition. Pure and Applied Mathematics (Amsterdam), 140. Elsevier/Academic Press, Amsterdam, 2003.
- [3] M.S. ALNÆS, J. BLECHTA, J. HAKE, A. JOHANSSON, B. KEHLET, A. LOGG, C. RICHARDSON, J. RING, M.E. ROGNES, AND G.N. WELLS, *The FEniCS project version 1.5*. *Arch. Numer. Softw.*, 3(100) (2015) 9–23.
- [4] M. AMARA, D. CAPATINA-PAPAGHIUC, AND D. TRUJILLO, *Stabilized finite element method for Navier–Stokes equations with physical boundary conditions*. *Math. Comp.*, 76(259) (2007) 1195–1217.
- [5] M. AMARA, E. CHACÓN VERA, AND D. TRUJILLO, *Vorticity–velocity–pressure formulation for Stokes problem*. *Math. Comp.*, 73(248) (2004) 1673–1697.
- [6] P.R. AMESTOY, I.S. DUFF, AND J.-Y. L’EXCELLENT, *Multifrontal parallel distributed symmetric and unsymmetric solvers*. *Comput. Methods Appl. Mech. Engrg.*, 184 (2000) 501–520.
- [7] K. AMOURA, M. AZAÏEZ, C. BERNARDI, N. CHORFI, AND S. SAADI, *Spectral element discretization of the vorticity, velocity and pressure formulation of the Navier–Stokes problem*. *Calcolo*, 44(3) (2007) 165–188.
- [8] V. ANAYA, A. BOUHARGUANE, D. MORA, C. REALES, R. RUIZ-BAIER, N. SELOULA AND H. TORRES, *Analysis and approximation of a vorticity-velocity-pressure formulation for the Oseen equations*. *J. Sci. Comput.*, 88(3) (2019) 1577–1606.
- [9] V. ANAYA, R. CARABALLO, B. GÓMEZ-VARGAS, D. MORA, AND R. RUIZ-BAIER, *Velocity-vorticity-pressure formulation for the Oseen problem with variable viscosity*. *Calcolo*, 58(4) (2021) e44(1–25).
- [10] V. ANAYA, G.N. GATICA, D. MORA, AND R. RUIZ-BAIER, *An augmented velocity-vorticity-pressure formulation for the Brinkman equations*. *Int. J. Numer. Meth. Fluids*, 79(3) (2015) 109–137.
- [11] V. ANAYA, B. GÓMEZ-VARGAS, D. MORA, AND R. RUIZ-BAIER, *Incorporating variable viscosity in vorticity-based formulations for Brinkman equations*. *Compt. Rend. Math.*, 357(6) (2019) 552–560.
- [12] V. ANAYA, D. MORA, R. OYARZÚA, AND R. RUIZ-BAIER, *A priori and a posteriori error analysis of a mixed scheme for the Brinkman problem*. *Numer. Math.*, 133(4) (2016) 781–817.
- [13] V. ANAYA, D. MORA, AND R. RUIZ-BAIER, *An augmented mixed finite element method for the vorticity-velocity-pressure formulation of the Stokes equations*. *Comput. Methods Appl. Mech. Engrg.*, 267 (2013) 261–274.
- [14] D.N. ARNOLD, F. BREZZI, AND M. FORTIN, *A stable finite element for the Stokes equations*. *Calcolo*, 21 (1984) 337–344.
- [15] M. AZAÏEZ, C. BERNARDI, AND N. CHORFI, *Spectral discretization of the vorticity, velocity and pressure formulation of the Navier–Stokes equations*. *Numer. Math.*, 104(1) (2006) 1–26.
- [16] M. BENZI, M.A. OLSHANSKII, L.G. REBHOLZ, AND Z. WANG, *Assessment of a vorticity based solver for the Navier–Stokes equations*. *Comput. Methods Appl. Mech. Engrg.*, 247–248 (2012) 216–225.
- [17] C. BERNARDI, AND N. CHORFI, *Spectral discretization of the vorticity, velocity, and pressure formulation of the Stokes problem*. *SIAM J. Numer. Anal.*, 44(2) (2007) 826–850.
- [18] C. BERNARDI, S. DIB, V. GIRAULT, F. HECHT, F. MURAT, AND T. SAYAH, *Finite element methods for Darcy’s problem coupled with the heat equation*. *Numer. Math.*, 139 (2018) 315–348.
- [19] C. BERNARDI, AND G. RAUGEL, *Analysis of some finite elements for the Stokes problem*. *Math. Comput.*, 44 (1985) 71–79.
- [20] P.V. BOCHEV, *Analysis of least-squares finite element methods for the Navier–Stokes equations*. *SIAM J. Numer. Anal.*, 34(5) (1997) 1817–1844.
- [21] P.B. BOCHEV, *Negative norm least-squares methods for the velocity-vorticity-pressure Navier–Stokes equations*. *Numer. Methods PDEs*, 15 (1999) 237–256.
- [22] D. BOFFI, F. BREZZI, AND M. FORTIN, *Mixed Finite Element Methods and applications*. Springer Series in Computational Mathematics, 44. Springer, Heidelberg (2013).
- [23] C.L. CHANG, AND B.-N. JIANG, *An error analysis of least-squares finite element method of velocity-pressure-vorticity formulation for the Stokes problem*. *Comput. Methods Appl. Mech. Engrg.*, 84(3) (1990) 247–255.

- [24] B. COCKBURN, AND J. CUI, *An analysis of HDG methods for the vorticity-velocity-pressure formulation of the Stokes problem in three dimensions*. *Math. Comp.*, 81(279) (2012) 1355–1368.
- [25] M. CROUZEIX, AND P.-A. RAVIART, *Conforming and nonconforming finite element methods for solving the stationary Stokes equations I*. *ESAIM: Math. Model. Numer. Anal.*, 7 (1973) 33–75.
- [26] Y. DAIKH AND D. YAKOUBI, *Spectral discretization of the Navier–Stokes problem with mixed boundary conditions*. *Appl. Numer. Math.*, 118 (2017) 33–49.
- [27] H.-Y. DUAN, AND G.-P. LIANG, *On the velocity-pressure-vorticity least-squares mixed finite element method for the 3D Stokes equations*. *SIAM J. Numer. Anal.*, 41(6) (2003) 2114–2130.
- [28] F. DUBOIS, M. SALAÜN, AND S. SALMON, *First vorticity-velocity-pressure numerical scheme for the Stokes problem*. *Comput. Methods Appl. Mech. Engrg.*, 192(44–46) (2003) 4877–4907.
- [29] A. ERN, *Vorticity-velocity formulation of the Stokes problem with variable density and viscosity*. *Math. Models Methods Appl. Sci.*, 8(2) (1998) 203–218.
- [30] G.N. GATICA, *A Simple Introduction to the Mixed Finite Element Method. Theory and Applications*. Springer Briefs in Mathematics, Springer, Cham Heidelberg New York Dordrecht London (2014).
- [31] G.N. GATICA, R. OYARZÚA, AND N. VALENZUELA, *A five-field augmented fully-mixed finite element method for the Navier–Stokes/Darcy coupled problem*. *Compu. Math. Appl.*, 80(8) (2020) 1944–1963.
- [32] C. GEUZAINÉ, AND J.-F. REMACLE, *Gmsh: a three-dimensional finite element mesh generator with built-in pre- and post-processing facilities*. *Int. J. Numer. Meth. Engrg.*, 79 (2009) 1309–1331.
- [33] V. GIRAULT, AND P.A. RAVIART, *Finite element methods for Navier–Stokes equations. Theory and algorithms*. Springer-Verlag, Berlin (1986).
- [34] F. HECHT, *New development in FreeFem++*, *J. Numer. Math.*, 20(3-4) (2012) 251–265.
- [35] P. HOOD, AND C. TAYLOR, *Numerical solution of the Navier–Stokes equations using the finite element technique*. *Comput. Fluids*, 1 (1973) 1–28.
- [36] W. LAYTON, C.C. MANICA, M. NEDA, M. OLSHANSKII, AND L.G. REBHOLZ, *On the accuracy of the rotation form in simulations of the Navier–Stokes equations*. *J. Comput. Phys.*, 228(9) (2009) 3433–3447.
- [37] A. LINKE, AND C. MERDON, *Pressure-robustness and discrete Helmholtz projectors in mixed finite element methods for the incompressible Navier–Stokes equations*. *Comput. Methods Appl. Mech. Engrg.*, 311 (2016) 304–326.
- [38] M.A. OLSHANSKII, AND A. REUSKEN, *Navier–Stokes equations in rotation form: a robust multigrid solver for the velocity problem*. *SIAM J. Sci. Comput.*, 23(5) (2002) 1683–1706.
- [39] P.R. PATIL, AND G. VAIDYANATHAN, *Effect of variable viscosity on thermohaline convection in a porous medium*. *J. Hydrology*, 57(1-2) (1982) 147–161.
- [40] L.E. PAYNE, AND B. STRAUGHAN, *Convergence and continuous dependence for the Brinkman-Forchheimer equations*. *Stud. Appl. Math.*, 102(4) (1999) 419–439.
- [41] A. QUARTERONI, AND A. VALLI, *Numerical Approximation for Partial Differential Equations*. Springer-Verlag Berlin, 2009.
- [42] J. RUDI, G. STADLER, AND O. GHATTAS, *Weighted BFBT preconditioner for Stokes flow problems with highly heterogeneous viscosity*. *SIAM J. Sci. Comput.*, 39(5) (2017) S272–S297.
- [43] M. SALAÜN, AND S. SALMON, *Numerical stabilization of the Stokes problem in vorticity-velocity-pressure formulation*. *Comput. Methods Appl. Mech. Engrg.*, 196(9-12) (2007) 1767–1786.
- [44] M. SALAÜN, AND S. SALMON, *Low-order finite element method for the well-posed bidimensional Stokes problem*. *IMA J. Numer. Anal.*, 35 (2015) 427–453.
- [45] C.-C. TSAI, AND S.-Y. YANG, *On the velocity-vorticity-pressure least-squares finite element method for the stationary incompressible Oseen problem*. *J. Comput. Appl. Math.*, 182(1) (2005) 211–232.
- [46] P.S. VASSILEVSKI, AND U. VILLA, *A mixed formulation for the Brinkman problem*. *SIAM J. Numer. Anal.*, 52(1) (2014) 258–281.